MASARYKOVA UNIVERZITA
Přírodovědecká fakulta
Ústav teoretické fyziky a astrofyziky

BAKALÁŘSKÁ PRÁCE

Růst supermasivních černých děr v nesrážejících se galaxiích

Lenka Josefína Sládková

Vedoucí: Izzy L. Garland, Ph. D.

Brno 2025

Bibliografický záznam

Autor:	Lenka Josefína Sládková Přírodovědecká fakulta, Masarykova univerzita Ústav teoretické fyziky a astrofyziky

Název práce:	Růst supermasivních černých děr v nesrážejících se galaxiích
Studijní program:	Fyzika
Studijní obor:	Astrofyzika
Vedoucí práce:	Izzy L. Garland, Ph. D.
Akademický rok:	2025/2026
Počet stran:	IX + 60
Klíčová slova:	Supermasivní černé díry, aktivní galaktická jádra, morfologie galaxií, galaktické příčky

Bibliographic Record

Author:	Lenka Josefína Sládková Faculty of Science, Masaryk University Department of Theoretical Physics and Astrophysics

Thesis title:	Supermassive Black Hole Growth in the Absence of Mergers
Study programme:	Physics
Field of study:	Astrophysics
Supervisor:	Izzy L. Garland, Ph. D.
Academic year:	2025/2026
Number of pages:	IX + 60
Keywords:	Supermassive black holes, active galactic nuclei, galaxy morphology, galactic bars

Abstract:
Supermassive black holes (SMBHs) are known to correlate with host-galaxy properties, often interpreted as evidence for merger-driven co-evolution. However, many nearby disc-dominated galaxies lack signatures of major mergers while still hosting actively accreting SMBHs, providing a means to study secular growth processes.

In this thesis, we examine whether large-scale stellar bars influence SMBH growth in disc-dominated, merger-free galaxies hosting Type 1, unobscured active galactic nuclei (AGN). Using a sample of disc galaxies hosting Type 1 AGN with little to no bulge component, together with follow-up spectroscopy and high-resolution *HST* imaging, we investigate the relationships between bar strength, black hole mass, and bolometric luminosity. We find no significant correlation between bar strength and black hole mass, but identify a moderate negative correlation between bar strength and bolometric luminosity.

Abstrakt:
Supermasivní černé díry (SMBH) jsou známy tím, že korelují s vlastnostmi svých hostitelských galaxií, což je často interpretováno jako důkaz koevoluce řízené galaktickými srážkami. Řada blízkých diskových galaxií však postrádá známky významných srážek, přesto hostí aktivně akreující SMBH, což umožňuje studium sekulárních procesů růstu.

V této práci zkoumáme vliv galaktických příček na růst supermasivních černých děr v diskových galaxiích bez významných srážek, které hostí nezakrytá aktivní galaktická jádra (AGN) typu 1. Na základě vzorku diskových galaxií s AGN typu 1 s minimální nebo žádnou výdutí, doplněného o následnou spektroskopii a vysokorozlišovací snímky z dalekohledu *HST*, analyzujeme vztahy mezi silou příčky, hmotností černé díry a bolometrickou svítivostí. Nezjišťujeme žádnou významnou korelaci mezi silou příčky a hmotností černé díry, avšak nacházíme mírnou negativní korelaci mezi silou příčky a bolometrickou svítivostí.

MUNI
SCI

MASARYKOVA UNIVERZITA
PŘÍRODOVĚDECKÁ FAKULTA
KOTLÁŘSKÁ 2, 611 37 BRNO
IČ: 00216224
DIČ: CZ00216224

ZADÁNÍ BAKALÁŘSKÉ PRÁCE

Akademický rok: 2025/2026

Ústav:	Ústav teoretické fyziky a astrofyziky
Studentka:	Lenka Josefína Sládková
Program:	Fyzika
Specializace:	Astrofyzika

Ředitel *ústavu* PřF MU Vám ve smyslu Studijního a zkušebního řádu MU určuje bakalářskou práci s názvem:

Název práce:	Růst supermasivních černých děr v nesrážejících se galaxiích
Název práce anglicky:	Supermassive Black Hole Growth in the Absence of Mergers
Jazyk práce:	angličtina

Oficiální zadání:
Co-evolution between supermassive black holes (SMBH) and their host galaxies is observed via several relationships between SMBH properties and galaxy properties. However, the origin of these relationships is not well understood. Mergers are understood to be one cause, but in the last few years, simulations have shown that the majority of SMBH growth since redshift~3 has occurred via secular processes (*i.e.*, in the absence of mergers). Merger-free growth can be traced observationally via galaxy morphology, since disk-dominated galaxies with a small bulge to total stellar mass ratio have evolved via merger-free pathways since redshift~2. Thus, by investigating active galactic nuclei (AGN, rapidly accreting SMBHs) in disk-dominated galaxies at low redshift, this merger-free growth can be investigated.
The student will use observations made by various facilities and surveys (such as SDSS, HST and Lick Observatory) to analyse samples of AGN in disk-dominated hosts. Since stellar dynamics are incredibly challenging to observe directly, requiring many on-sky observing hours, the student will use galaxy morphologies as tracers of these stellar dynamics with the aim of understanding the interplay between various morphological features and AGN presence. They will use python (and the comprehensive libraries within) to investigate the host-AGN correlation in further detail and develop theories about the co-evolution from their results.

Fahey M., Garland I. L., et al., 2025, MNRAS, 537, 3511
Garland I. L., et al., 2023, MNRAS, 522, 211
Garland I. L., et al., 2024, MNRAS, 532, 2320
Häring N., Rix H.-W., 2004, ApJ, 604, L89
Simmons B. D., Smethurst R. J., Lintott C., 2017, MNRAS, 470, 1559
Martin G. et al., 2018, MNRAS, 476, 2801
Martig M., Bournaud F., Croton D. J., Dekel A., Teyssier R., 2012, ApJ, 756, 26

Vedoucí práce:	Isobelle Lilian Mary Garland, Ph.D
Konzultant:	doc. RNDr. Michal Zajaček, Dr. rer. nat.
Datum zadání práce:	26. 3. 2025
V Brně dne:	12. 5. 2026

Zadání bylo schváleno prostřednictvím IS MU.

Lenka Josefína Sládková, 20. 11. 2025
Isobelle Lilian Mary Garland, Ph.D, 26. 3. 2025
Mgr. Michael Krbek, Ph.D., 17. 3. 2026

Acknowledgements: I would like to express my sincere gratitude to my supervisor, Izzy L. Garland, Ph. D., for their outstanding guidance and support throughout this thesis.

They devoted a remarkable amount of time to reading and commenting on multiple drafts of this work, providing thorough and insightful suggestions that significantly improved both the scientific content and the overall clarity of the thesis. I am particularly thankful for their encouragement and patience, which helped me stay motivated and confident throughout the project. Their willingness engage deeply with the project, even outside regular working periods, was invaluable.

Beyond their academic guidance, I am grateful for the positive and supportive working environment they fostered, which made this project both intellectually stimulating and personally rewarding. This thesis would not have been possible without their generosity and unwavering support, and I am very grateful for the opportunity to have worked under their supervision.

I would also like to acknowledge the observational data that formed the basis of this work. This thesis makes use of data from the Sloan Digital Sky Survey III (SDSS-III), which is credited as follows:

Funding for SDSS-III has been provided by the Alfred P. Sloan Foundation, the Participating Institutions, the National Science Foundation, and the U.S. Department of Energy Office of Science. The SDSS-III web site is http://www.sdss3.org/. SDSS-III is managed by the Astrophysical Research Consortium for the Participating Institutions of the SDSS-III Collaboration including the University of Arizona, the Brazilian Participation Group, Brookhaven National Laboratory, Carnegie Mellon University, University of Florida, the French Participation Group, the German Participation Group, Harvard University, the Instituto de Astrofisica de Canarias, the Michigan State/Notre Dame/JINA Participation Group, Johns Hopkins University, Lawrence Berkeley National Laboratory, Max Planck Institute for Astrophysics, Max Planck Institute for Extraterrestrial Physics, New Mexico State University, New York University, Ohio State University, Pennsylvania State University, University of Portsmouth, Princeton University, the Spanish Participation Group, University of Tokyo, University of Utah, Vanderbilt University, University of Virginia, University of Washington, and Yale University.

Prohlašuji, že jsem tuto bakalářskou práci vypracovala samostatně a výhradně s použitím citovaných zdrojů.

V Brně dne 5. ledna 2026 Lenka Josefína Sládková

Contents

Chapter 1

Introduction

Supermassive black holes (SMBHs) are now known to reside at the centres of most massive galaxies and to correlate tightly with several host-galaxy properties. These scaling relations are often interpreted as evidence for a coupled evolutionary history in which black holes and their host galaxies grow alongside each other [Shankar et al., 2020]. In the conventional framework, major mergers are thought to play a dominant role in galaxy evolution. They drive violent inflows of gas, trigger intense starbursts and fuel luminous active galactic nuclei (AGN), thereby contributing to the growth of both bulges and central black holes.

Since major mergers tend to destroy stellar discs and produce prominent, dispersion-supported bulges, galaxies lacking a classical bulge are generally understood to have avoided significant merger events (see Section 2.1.1). However, many nearby galaxies are strongly disc-dominated and show little or no sign of a classical bulge, yet still host actively accreting SMBHs. This raises a key question: how do supermassive black holes grow in galaxies that have evolved without major mergers? [Barnes et al., 1991, Simmons et al., 2017]

Secular processes are slow, internal evolutionary processes in galaxies, driven by structures like bars and spiral arms rather than by galaxy mergers. In merger-free systems, secular processes must dominate the evolution of both the stellar disc and the central black hole. Non-axisymmetric structures—in particular large-scale stellar bars—are especially important in this context. Bars redistribute angular momentum, rearrange disc material into rings and central concentrations, and are theoretically expected to drive gas inwards toward the central kiloparsec [Sellwood and Wilkinson, 1993, Kormendy and Kennicutt, 2004]. This bar-driven inflow can, in principle, both build pseudobulges (Section

2.1.1) and supply gas to fuel AGN activity. Yet, despite decades of theoretical and numerical work on bar dynamics, observational constraints on how bar strength relates to SMBH growth in clearly merger-free galaxies remain limited. Previous studies have often been hampered by small samples or uncertain black hole mass estimates.

Disc-dominated AGN hosts provide an ideal laboratory for isolating secular growth channels. These galaxies lack massive classical bulges and show no evidence of recent major mergers, implying that any substantial SMBH growth must have occurred through internal processes such as bar- or spiral-driven inflows. At the same time, Type 1 (unobscured) AGN in these systems offer direct access to broad emission lines whose widths and luminosities can be used to estimate black hole masses via single-epoch virial methods [Greene and Ho, 2005]. This makes it possible to examine whether the properties of the central black hole correlate with the strength of the bar in the surrounding disc.

The central aim of this thesis is to investigate whether bar strength influences SMBH growth in disc-dominated, non-merger galaxies hosting Type 1 AGN. More specifically, we address the following questions:

1. How does black hole mass in disc-dominated, merger-free AGN hosts relate to the strength of their large-scale stellar bars?

2. Does bar strength correlate with bolometric luminosity, and therefore with the current accretion rate onto the SMBH?

In other words, the goal is to test whether stronger bars are associated with more massive black holes, more actively accreting black holes, neither, or both.

To address these questions, we use the disc-dominated Type 1 AGN sample introduced by [Simmons et al., 2017], consisting of galaxies with little or no bulge and no evidence for major mergers, which are ideal for studying secular evolution. This sample is supplemented with follow-up spectroscopy from the Shane 3 m Telescope at Lick Observatory [Garland et al., 2023] and high-resolution *HST* imaging with detailed structural decompositions [Fahey et al., 2025]. These datasets provide reliable broad-line measurements for virial black hole mass estimates and quantitative bar parameters from `GALFIT` modelling.

The remainder of this thesis is organised as follows. Chapter 2 reviews the theoretical background on supermassive black holes, AGN, galactic morphology, barred galaxies, and secular evolution, and introduces the virial method used for black hole mass estimation. Chapter 3 describes the observational datasets employed in this work, including the SDSS, Lick, and *HST* samples, and the

construction of the disc-dominated AGN host sample. Chapter 4 details the derivation of emission-line and structural parameters, the Hα-based black hole mass estimates, and the bar-strength metric. The main results, including the relationships between bar strength, black hole mass, and bolometric luminosity, are presented in Chapter 5. Chapter 6 discusses the implications of these findings for SMBH growth in merger-free galaxies. Prospects for future work are discussed in Chapter 7.

Chapter 2

Theoretical Background

2.1 Galaxies

Galaxies are some of the most complex structures in the Universe, encompassing a wide range of masses, morphologies, and evolutionary histories. At a fundamental level, a galaxy may be formally defined as "a gravitationally bound collection of stars whose properties cannot be explained by a combination of baryons and Newton's laws of gravity" [Willman and Strader, 2012]. This definition distinguishes galaxies from smaller stellar systems by requiring dynamical properties that cannot be explained by baryonic matter under Newtonian gravity, a criterion that in standard cosmological models is typically associated with the presence of dark matter. Since AGN activity is intimately linked to the large-scale structure of their host galaxies, we next review the main morphological classes of galaxies and the structural features relevant to black hole fuelling [Willman and Strader, 2012].

2.1.1 Galactic structures: bulges, pseudobulges, and bars

Classical Bulges and Pseudobulges

Bulges are dense central stellar components commonly found in disc galaxies, but observations and theoretical work indicate that they can form through distinct evolutionary pathways. Classical bulges are thought to originate from rapid and violent processes, such as early dissipative collapse and galaxy mergers, which dominate galaxy evolution at early cosmic times [Eggen et al., 1962, Toomre, 1977, Sandage, 1990]. These processes produce dynamically hot, spheroidal struc-

tures resembling elliptical galaxies. A visual illustration of a galactic bulge embedded within a stellar disc is shown in Figure2.1.

In contrast, pseudobulges are central components that form more gradually from disc material rather than through mergers [Kormendy and Kennicutt, 2004]. Although pseudobulges can appear similar to classical bulges in surface brightness, they retain clear signatures of their disc origin. Observationally, pseudobulges tend to be flatter, show higher levels of rotational support, and exhibit lower central velocity dispersions than expected for classical bulges of similar luminosity [Kormendy and Gebhardt, 2001, Kormendy and Kennicutt, 2004]. They often display nearly exponential surface brightness profiles and may contain nuclear spirals, nuclear bars, or ongoing central star formation [Courteau, 1996, Carollo, 1999].

The coexistence of classical bulges, pseudobulges, and even bulgeless disc galaxies in the present-day Universe demonstrates the diversity of bulge formation, highlighting the importance of internal processes in shaping the central regions of disc galaxies[Kormendy and Kennicutt, 2004]. Because major mergers efficiently disrupt stellar discs and build dispersion-supported classical bulges, the absence of a classical bulge is therefore commonly interpreted as evidence that a galaxy has not experienced a major merger.

Galactic Bars

Galactic bars are very common structural features in disc galaxies. Near-infrared observational studies show that a large fraction of disc galaxies host bars, with 56% classified as strongly barred and an additional 16% as weakly barred [Eskridge et al., 2000]. In optical wavelengths, this number is closer to 30% [Masters et al., 2010]. Bars display a wide range of morphologies, varying in length, thickness, and shape, from thin and elongated to short and boxy or peanut-like structures.

Bars undergo significant changes in shape as they evolve. Numerical simulations show that bars tend to grow longer and more symmetric over time, and that ring-like structures can develop around them, similar to the inner rings observed in many barred galaxies [Buta, 1987]. When galaxies are viewed edge-on, bars also thicken vertically and appear boxy or peanut-shaped. Observations indicate that these boxy or peanut-shaped structures are not separate bulges, but rather bars seen from an edge-on perspective [Contopoulos and Papayannopoulos, 1980]. This behaviour illustrates the strong link between bar evolution and the three-dimensional structure of disc galaxies.

Figure 2.1: **Artist's impression of the central bulge of the Milky Way.** The central bulge appears as a bright, dense concentration of stars at the galaxy's centre, embedded within the flattened stellar disc. From this perspective, the disc and spiral arms form a thin band intersected by dust lanes, while the bulge dominates the central light distribution. The image provides a visual illustration of a galactic bulge as discussed in Section 2.1.1 (Image source: [ESO, 2013]).

The evolution of bars is driven by the redistribution of angular momentum within the galaxy. Angular momentum is mainly emitted by material near resonances within the bar region and absorbed by resonant material in the outer disc and the dark matter halo [Lynden-Bell and Kalnajs, 1972, Athanassoula, 2003]. As the bar loses angular momentum, it becomes stronger and its rotation slows down. The dark matter halo plays an important role in this process, as it can absorb a substantial amount of angular momentum despite being dynamically hotter than the stellar disc [Athanassoula, 2003].

2.1.2 Morphological Classification of Galaxies

Galaxies can be systematically divided into various types on the basis of their appearance or their integrated spectra [Binney and Merrifield, 1998]. The most widely used appearance-based morphological classification system is the *Hubble sequence*, which groups galaxies into ellipticals (E), spirals (S), and irregular (Irr). Spirals are further divided into normal (S) and barred (SB) types, and lenticular galaxies (S0) form a transitional class between ellipticals and spirals.

These categories are organised in Hubble's well-known *tuning-fork diagram*, as seen in Figure 2.2, which he mistakenly interpreted as an evolutionary sequence, giving rise to the terms *early-type* and *late-type* galaxies [Kormendy and Bender, 1996, Carroll and Ostlie, 2017]. Beyond the standard Hubble classification, alternative schemes—particularly the de Vaucouleurs system—incorporate the symbols *(r)* and *(s)* to distinguish galaxies that exhibit ring structures from those that do not [Binney and Merrifield, 1998].

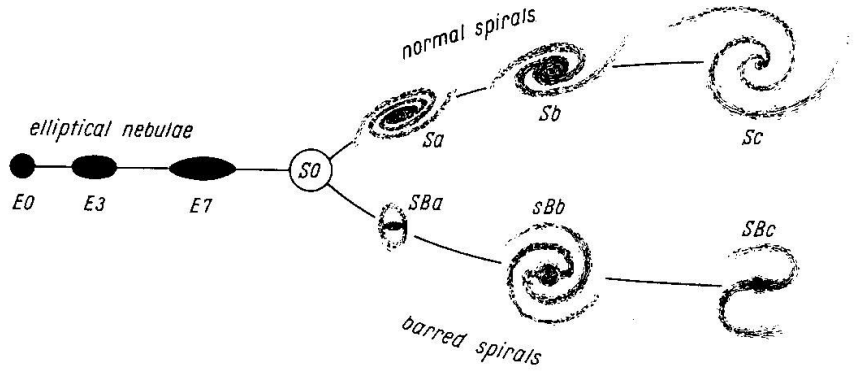

Figure 2.2: **Schematic representation of the Hubble galaxy morphological classification sequence.** Galaxies are arranged along the so-called Hubble sequence according to their visual morphology, ranging from elliptical galaxies (E0–E7) on the left to spiral galaxies on the right. Spiral galaxies are subdivided into normal spirals (Sa–Sc), characterised by increasingly open spiral arms and decreasing bulge prominence, and barred spirals (SBa–SBc), which exhibit a central stellar bar. Lenticular galaxies (S0) occupy an intermediate position between ellipticals and spirals. This classification is based purely on morphology and does not represent an evolutionary sequence [Hubble, 1936, Kormendy and Bender, 1996]

.

2.1.3 Subclassifications of Spiral Galaxies

According to Fix [2007], approximately 80% of galaxies in the local Universe are observed to be disc-dominated systems, most of which are classified as spiral galaxies. A normal spiral galaxy consists of a bright central concentration similar in appearance to an elliptical galaxy, embedded within a thin disc. This disc contains spiral patterns of increased brightness, known as spiral arms. In barred

spiral galaxies, a linear bar structure is present inside the region occupied by the spiral arms. This bar often includes dark lanes, which are thought to result from dust absorbing starlight. In such galaxies, the spiral arms usually originate at the ends of the bar. Both normal and barred spirals are further subdivided into subclasses. These subdivisions are defined using a combination of three classification criteria. The first criterion concerns the relative prominence of the central luminous bulge and the role the outer disc plays in shaping the galaxy's overall light distribution. Additional classification criteria include how tightly the spiral arms are wound and how distinctly they can be resolved into individual stars. Although this combination of criteria may seem unsatisfactory at first, it is supported by the fact that these properties are strongly correlated. In particular, galaxies with prominent central bulges tend to display tightly wound spiral arms that are not well resolved into stars. As a result, astronomers independently classifying galaxies usually arrive at very similar type assignments [de Vaucouleurs, 1959, 1963, Binney and Merrifield, 1998].

Early-type spiral galaxies—located toward the left side of the Hubble diagram, are characterised by large, bright central bulges and smooth, tightly wound spiral arms. These galaxies are classified as Sa or SBa, depending on whether they are unbarred or barred. In contrast, late-type spirals have smaller central brightness concentrations and loosely wound arms that are highly resolved into stars; these systems are designated Sc or SBc. Galaxies with intermediate properties fall into the Sb and SBb classes. Intermediate stages of bulge prominence and arm tightness are labelled Sab, Sbc, and related types [Binney and Merrifield, 1998].

2.1.4 Barred Spiral galaxies

Barred galaxies form a large and diverse subset of disc galaxies, with near-infrared observations revealing that approximately 60% of luminous disc galaxies contain a bar [Oh et al., 2012]. Classical catalogues, largely based on optical classifications, generally find that strongly barred galaxies constitute roughly one-quarter to one-third of disc galaxies. However, infrared observations reveal additional bars in systems classified as unbarred at optical wavelengths, suggesting that the true bar fraction is likely higher [Sellwood and Wilkinson, 1993]. Bars that vary widely in strength, size, and associated structures such as rings, spiral arms, dust lanes, and central gas concentrations. Bars occur across the full range of disc morphologies in the Hubble sequence, and their apparent strengths form a continuous distribution, from weak oval distortions to strong, elongated

bars, making the boundary between barred and unbarred systems partly subjective [Oh et al., 2012]. Ellipticals, despite sometimes appearing elongated, lack the disc–bulge structure of barred spirals and are not included in this category [Sellwood and Wilkinson, 1993]. A schematic illustration of the main structural components of a barred spiral galaxy is shown in Figure2.3.

The light distribution of barred galaxies is commonly decomposed into disc, bulge, and bar components, although quantitative separation remains challenging. In the inner regions, the mass is dominated by stars, with gas acting mainly as a tracer, while dark matter becomes dynamically important only in the outer disc. Barred galaxies are dynamically evolved systems whose long-lived stellar orbits indicate structures shaped by slow, secular processes rather than by short-lived transients. Their morphology, including rings, lenses, and central concentrations, is broadly consistent with theoretical expectations for evolution driven by non-axisymmetric gravitational potentials [Sellwood and Wilkinson, 1993], [Kormendy and Kennicutt, 2004].

Because bars efficiently redistribute angular momentum, they can funnel gas toward the central regions of disc galaxies, contributing to circumnuclear star formation and the build-up of central gas reservoirs [Galloway et al., 2015, Silva-Lima et al., 2022]. These secular processes are particularly relevant for understanding merger-free pathways of galaxy evolution, as a significant fraction of AGN are hosted by disc-dominated systems with no recent major mergers [Garland et al., 2023]. In this context, bars represent plausible mechanisms for supplying gas to the central few hundred parsecs, potentially facilitating the fuelling of supermassive black holes, while additional dynamical processes are likely required to drive gas inflow on smaller scales [Silva-Lima et al., 2022].

2.1.5 Galaxy evolution

Galaxies are believed to originate from the gravitational collapse of very large gas clouds, initially much more extended than present-day galaxies. Interactions with neighbouring gas clouds imparted rotation to these systems through gravitational forces. Disc galaxies in particular appear to have conserved a large fraction of this initial angular momentum during their evolution.

In hierarchical models of structure formation, large galaxies grow through the accretion of smaller systems, making galaxy evolution a gradual process occurring over cosmic timescales [Carroll and Ostlie, 2017]. Galactic evolution can proceed through a range of pathways, including slow internal processes that shape galaxy structure and regulate star formation.

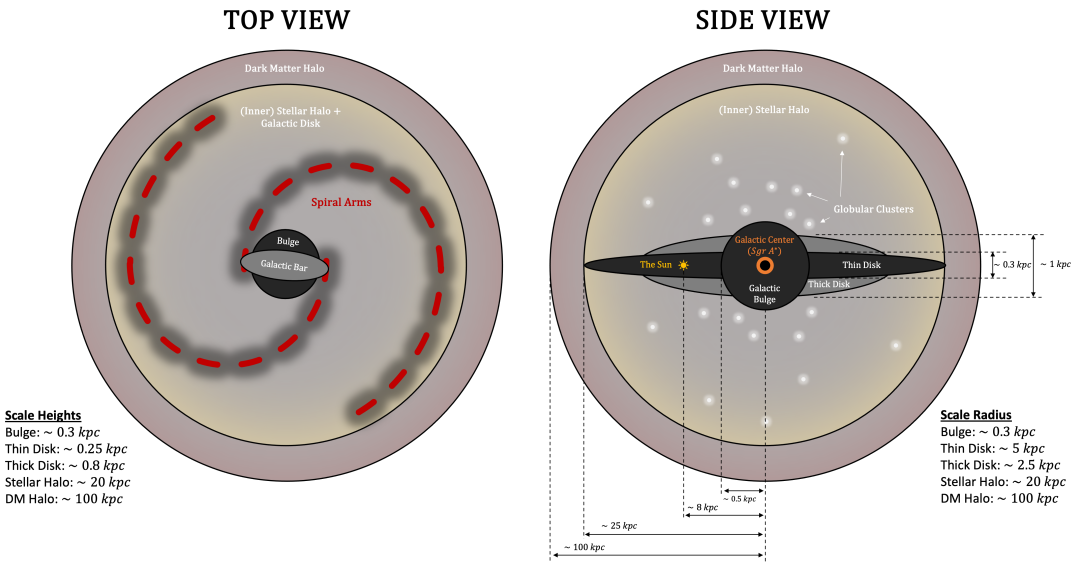

Figure 2.3: **Schematic representation of a typical barred spiral galaxy**. Illustrated here using the Milky Way as an example. The left panel shows a top-down view of the galaxy, highlighting the central stellar bar, spiral arms, galactic bulge, and extended stellar disc embedded within a dark matter halo. The right panel presents a side-on view, illustrating the vertical structure of the galaxy, including the thin and thick stellar discs, the bulge, the stellar halo, and the surrounding dark matter halo. Approximate characteristic spatial scales of the different components are indicated. This diagram emphasises the multi-component structure of barred spiral galaxies and the role of the central bar within the disc (Image source:[AstroWiki]).

Secular Evolution

Secular evolution describes the slow, internal rearrangement of mass and energy in galaxies, in contrast to the rapid, merger-driven evolution that dominated the early universe. As merger rates decline at low redshift, these long-timescale internal processes, operating far more slowly than the dynamical time, become increasingly important. Secular evolution is driven by interactions between stars or gas and large-scale non-axisymmetric structures such as bars, oval discs, spiral patterns, and triaxial halos, rather than by direct stellar encounters, which are too slow to have significant dynamical effects. It is effective across cosmic time, as suggested by galaxies that maintain thin, fragile discs yet show little or no bulge

component [Sellwood and Wilkinson, 1993, Kormendy and Kennicutt, 2004].

A major consequence of secular processes is the gradual formation of pseudobulges: dense central components built slowly from disc gas rather than through mergers. Simulations show that bars rearrange disc material into outer rings, inner rings, and central concentrations, efficiently funnelling gas to small radii where it reaches high densities that can fuel star formation. SB(s) morphology is favoured when the bar is weak or rapidly rotating, while SB(r) structure is associated with bars that have become stronger and slower through angular-momentum transport; the rarity of inflow-related dust lanes in SB(r) galaxies is consistent with this interpretation. Secular evolution is not limited to galaxies that are barred today, since bars can self-destruct after building up central mass concentrations, and global spiral structure can also drive slower but significant long-term evolution [de Vaucouleurs, 1959, 1963, Kormendy, 1979, Kormendy and Kennicutt, 2004].

Observationally, many barred and oval galaxies contain dense, actively star-forming centres with young stellar populations, supporting the secular formation of pseudobulges. These components retain clear signatures of their disc origin—flattened shapes, rotation-dominated kinematics, low velocity dispersions[1], exponential profiles, and nuclear spirals or bars—and they often host circumnuclear starbursts. Their formation on timescales of a few billion years, consistent with measured gas densities and star-formation rates, demonstrates that secular evolution is a viable and complementary pathway to hierarchical merging in building central galactic structure [Kormendy, 1979, Elmegreen and Elmegreen, 1985, Kormendy and Kennicutt, 2004].

Galaxy collisions

Galactic evolution is also influenced by gravitational encounters between galaxies, which can reshape galactic structure. Observations and numerical simulations have shown that interactions and mergers can significantly alter galaxy morphology and internal properties [Barnes et al., 1991]. Such events can trigger enhanced star formation and drive gas toward galactic centres, where it may contribute to luminous nuclear activity. As a result, major mergers have traditionally been viewed as an important mechanism driving galaxy evolution,

[1]Stellar velocity dispersion, σ, measures the typical random speeds of stars in a galaxy and is strongly correlated with the mass of the central supermassive black hole through the $M_{\rm BH}$–σ relation [Merritt and Ferrarese, 2001]. However, differences in how σ is measured can introduce systematic uncertainties in this relation [Merritt and Ferrarese, 2001].

as they can redistribute stars from rotation-supported discs into dispersion-supported bulges and ellipticals [Barnes et al., 1991]. SMBHs exhibit correlations with several host-galaxy properties, relations that have often been interpreted as evidence of merger-driven coevolution [Kormendy and Ho, 2013]. However, studies of moderate-luminosity AGN indicate that many such systems reside in disc-dominated galaxies with no enhanced merger incidence relative to inactive galaxies [Simmons et al., 2017]. In these hosts, significant black hole growth can occur without substantial bulge formation, suggesting the presence of merger-free growth channels [Simmons et al., 2017, Garland et al., 2023]. This work builds on this framework by examining how bar strength relates to SMBH mass in disc-dominated, merger-free systems.

2.2 Active Galactic Nuclei (AGN)

Many galaxies host unusually compact point-like sources at their centres, known as active galactic nuclei (AGN) [Binney and Merrifield, 1998]. More specifically, AGN are the luminous centres of galaxies in which a supermassive black hole, exceeding the mass of 10^5 solar masses, is actively accreting gas and dust [Netzer, 2015], producing intense radiation, jets, and winds capable of influencing the evolution of their host galaxies. These central engines can emit so much radiation that they dominate the total luminosity of their host galaxies [Binney and Merrifield, 1998]. As material spirals inward through the accretion disc, it becomes extremely hot and emits energy across the entire electromagnetic spectrum, from X-rays to radio wavelengths. In addition, if the black hole possesses angular momentum, electromagnetic processes may extract energy directly from its rotation [Urry and Padovani, 1995].

The multi-scale structure of AGN, from the central engine to large-scale jets, is illustrated in Figure 2.4. The main components of AGN and their observational classification are summarised in the unified model shown in Figure 2.5.

2.2.1 Supermassive Black Holes

Supermassive black holes (SMBHs) reside at the centres of nearly all large galaxies and contain masses ranging from several hundred thousand to many billions of solar masses, far exceeding those of stellar-mass black holes [Shankar et al., 2020]. Despite extensive observational evidence, their origins remain uncertain. The presence of extremely massive black holes in very distant galaxies indicates

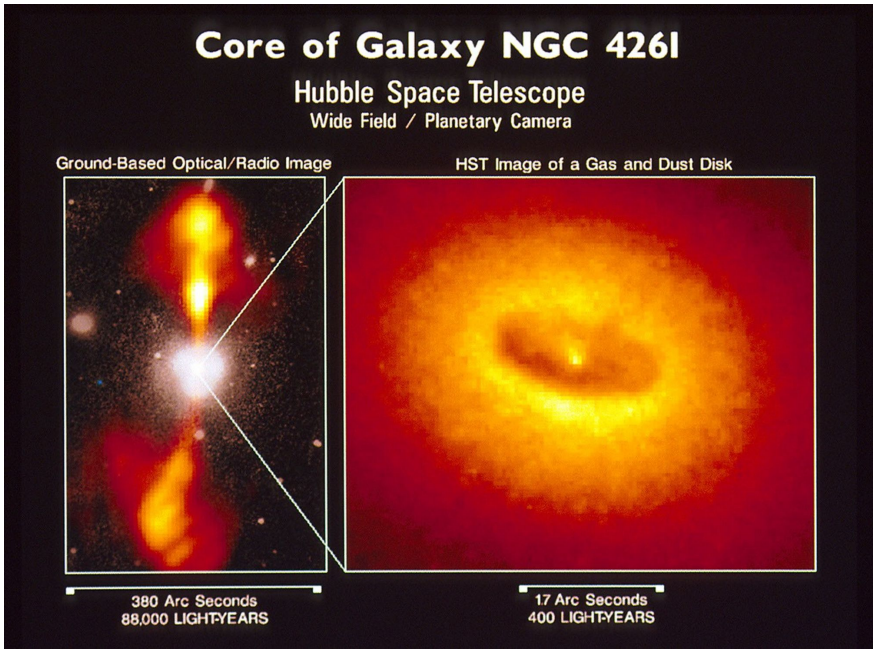

Figure 2.4: **Multi-scale view of the active galactic nucleus (AGN) in NGC 4261.** The left panel shows a ground-based optical and radio image, revealing large-scale radio jets extending tens of kiloparsecs from the galaxy centre. The right panel presents a high-resolution *Hubble Space Telescope* (HST) image of the central region, resolving a compact, rotating disc of gas and dust surrounding the nucleus on scales of a few hundred light-years. This circumnuclear structure is interpreted as the obscuring material invoked in unified models of AGN, feeding the central supermassive black hole while collimating the relativistic jets. The different spatial scales illustrated highlight the connection between small-scale accretion processes and large-scale jet activity (Image source: [NASA/ESA, 1997]).

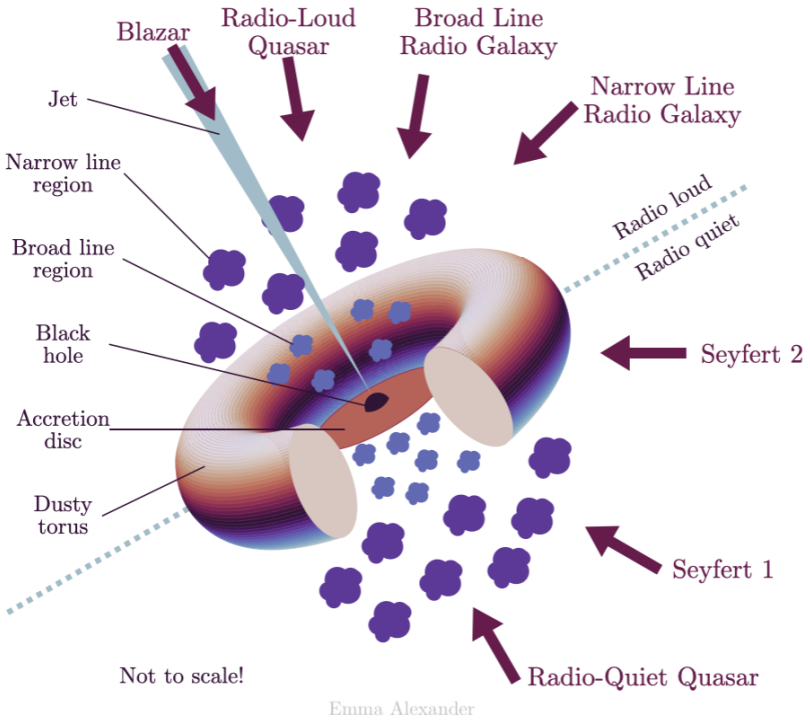

Figure 2.5: **Schematic illustration of the unified model of AGN.** The central engine consists of a supermassive black hole surrounded by an accretion disc, which produces intense optical, ultraviolet, and X-ray radiation. A dusty, geometrically thick torus obscures the central regions along certain lines of sight, while ionised gas located at different distances gives rise to the broad-line region (BLR) and narrow-line region (NLR). Relativistic jets may be launched perpendicular to the accretion disc, producing radio-loud AGN when oriented close to the observer's line of sight. The observed AGN class (e.g., Seyfert 1 and 2 galaxies, radio-quiet and radio-loud quasars, narrow-line and broad-line radio galaxies, and blazars) depends primarily on the viewing angle relative to the torus and jet axis, as well as on the presence or absence of strong radio emission. The diagram is not to scale [Urry and Padovani, 1995]. (Image source: [Alexander, 2022]).

that some SMBHs were already in place within the first billion years of cosmic history, implying rapid early growth. One possible explanation is that they formed from the collapse of unusually massive stars in the early universe, giving them a substantial initial mass from which to grow [Kormendy and Richstone,

1995, Kormendy and Ho, 2013].

Direct evidence for SMBHs comes from the motions of stars and gas in galactic centres. Dynamical mass estimates derived from stellar velocity dispersions or gas rotation curves reveal compact central objects with masses consistent with supermassive black holes. Such objects are found in both spiral and elliptical galaxies [Carroll and Ostlie, 2017].

SMBH masses also exhibit strong empirical correlations with global properties of their host galaxies. The most widely studied relations are those linking black hole mass to stellar mass and, even more strongly, to stellar velocity dispersion. In particular, SMBH mass scales approximately with the fourth or fifth power of the velocity dispersion, suggesting a close connection (or co-evolution) between galaxies and their central black holes. Analyses of the residuals in these relations indicate that velocity dispersion is the most fundamental predictor of black hole mass, with stellar mass playing a more secondary role. [Kormendy and Ho, 2013, Shankar et al., 2020].

Because different observational methods probe black hole masses over different ranges of luminosity and distance, studies often rely on AGN-based virial estimators, which allow masses to be measured even when the sphere of influence cannot be resolved. These techniques are discussed in detail in Section 2.3.

2.2.2 Types of AGN

According to Heckman and Best [2014], AGN in the local Universe can be broadly divided into two principal categories based on their dominant mode of energy output: radiative-mode AGN, in which most of the power is emitted as electromagnetic radiation through efficient accretion onto the central supermassive black hole, and jet-mode AGN, in which the primary energetic output is carried by collimated relativistic jets. Radiative-mode AGN include the traditionally defined Seyfert galaxies and quasi-stellar objects (QSOs). In this framework, Seyfert galaxies correspond to lower-luminosity radiative AGN, historically distinguished from QSOs primarily by luminosity and redshift rather than by intrinsic physical differences. Within this population, orientation effects give rise to Type 1 (unobscured) and Type 2 (obscured) AGN, as described by the unified model [Antonucci, 1993] (see Section 2.2.3). A small fraction of radiative-mode AGN are radio-loud and produce powerful jets. In contrast, jet-mode AGN, historically known as low-excitation radio galaxies, are associated with radiatively inefficient accretion flows such as advection-dominated accretion flows and radiatively inefficient accretion flows [Narayan and Yi, 1994, 1995, Narayan, 2005] and

are commonly classified as Fanaroff–Riley type I or II radio galaxies [Fanaroff and Riley, 1974]. At the lowest luminosities, low-ionisation nuclear emission-line regions populate the faint end of the AGN distribution, with the most powerful systems likely representing low-luminosity jet-mode AGN [Heckman and Best, 2014].

Considering the focus of this thesis, particular attention is given to the orientation-based classification of radiative-mode AGN. Type 1 AGN are observed from a line of sight close to the polar axis of the obscuring structure surrounding the central engine. From this viewing angle, there is a direct view of the supermassive black hole, the geometrically thin accretion disc, the hot corona, and the broad-line region. As a result, Type 1 AGN exhibit broad permitted emission lines, produced by dense gas clouds with velocity dispersions of several thousand km/s. Their optical, ultraviolet, and soft X-ray emission is directly observable. Type 2 AGN, on the other hand, are observed from a line of sight closer to the equatorial plane of the obscuring dusty molecular structure. In this orientation, the accretion disc, corona, and broad-line region are hidden from direct view. The presence of the AGN is instead inferred indirectly through thermal infrared emission from heated dust, hard X-rays that can penetrate the obscuring material, and narrow permitted and forbidden emission lines originating in the more extended narrow line region [Heckman and Best, 2014]. Permitted emission lines arise in relatively dense gas close to the central source, where common radiative transitions can occur efficiently and the gas motions are often dominated by rotation or gravity. In contrast, forbidden emission lines are produced in very diffuse gas, where particles are far enough apart for these weak transitions to occur, and they are commonly associated with outflowing material such as disc winds [Nemer and Goodman, 2024]. These emission lines are relatively narrow, indicating that the gas moves at speeds of only a few hundred kilometres per second [Heckman and Best, 2014]. A schematic classification of active galactic nuclei is shown on the Figure 2.6.

2.2.3 A Unified Model of AGN

Despite the wide variety of observed AGN types, evidence indicates that all are powered by the same basic mechanism: accretion onto a central supermassive black hole [Carroll and Ostlie, 2017]. As introduced earlier, a surrounding distribution of gas and dust can block radiation from the inner regions depending on the orientation of the observer [Urry and Padovani, 1995]. The observed diversity among AGN is therefore understood to arise largely from differences in

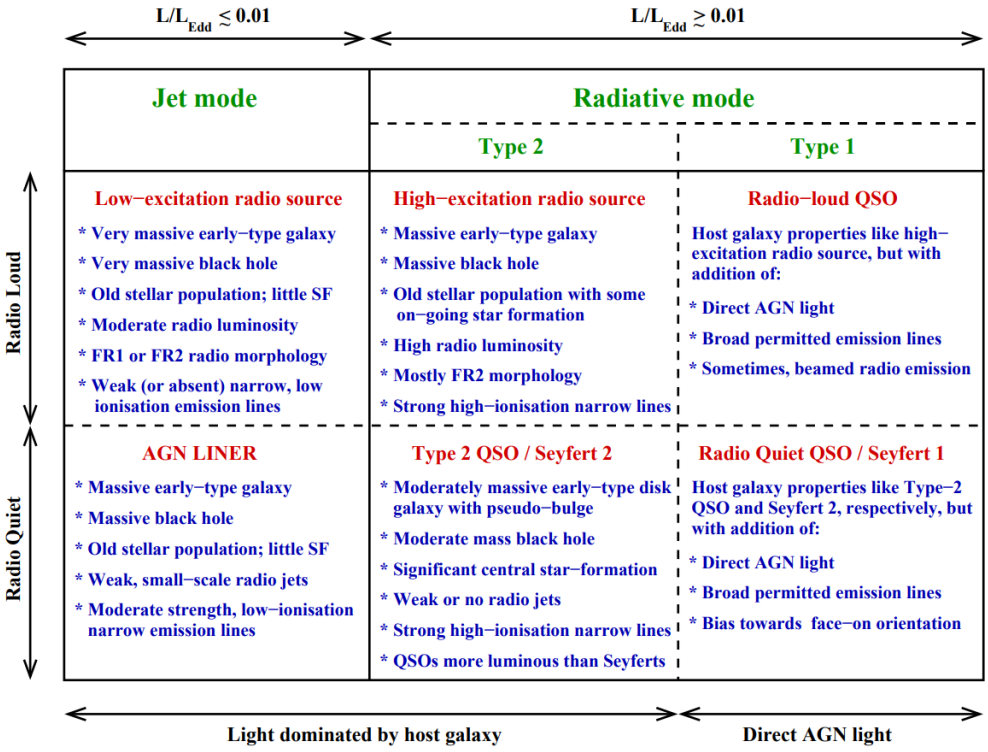

Figure 2.6: **Schematic classification of active galactic nuclei (AGN)** as a function of accretion mode, radiative efficiency, and radio properties. The diagram separates AGN into jet-mode systems at low Eddington ratios ($L/L_{\rm Edd} \lesssim 0.01$) and radiative-mode systems at higher Eddington ratios ($L/L_{\rm Edd} \gtrsim 0.01$). The vertical axis distinguishes radio-loud from radio-quiet AGN, while the horizontal axis indicates whether the observed emission is dominated by host-galaxy light or by direct AGN emission. Jet-mode AGN, often associated with radiatively inefficient accretion flows, include low-excitation radio galaxies and LINERs, and are characterised by weak ionising continua and prominent radio jets. Radiative-mode AGN are divided into Type 1 and Type 2 systems depending on orientation and obscuration, and include Seyfert galaxies and quasars, which exhibit strong optical emission lines and, in some cases, powerful radio emission. The figure illustrates how accretion state, radio activity, and orientation jointly determine the observed AGN class Heckman and Best [2014].

viewing angle, with additional contributions from variations in accretion rate and

black hole mass. A unified model of AGN is the hypothesis that the broad range of AGN observational properties can be primarily explained by differences in a restricted set of physical parameters [Netzer, 2015], and thus must explain why objects that are physically very similar can appear observationally very different.

To explain in more detail, the central engine is embedded within a complex environment composed of several gaseous components. Dense clouds moving at high velocities in the deep gravitational potential near the black hole give rise to broad optical and ultraviolet emission lines. At larger distances, more slowly moving gas produces emission lines with narrower profiles. Between these emitting regions and the observer lies an intervening distribution of gas and dust, often described as a toroidal or warped structure, which absorbs and blocks radiation along certain viewing directions [Urry and Padovani, 1995, Netzer, 2015]. AGN emission is therefore highly directional rather than uniform in all directions. Obscuration by dusty material prevents direct observation of the innermost regions along some lines of sight, whereas energetic outflows launched along the rotational axis form collimated jets. On small scales, plasma within these jets moves at relativistic speeds, causing radiation to be strongly enhanced in the direction of motion because of relativistic beaming. These effects introduce a pronounced dependence of the observed properties on the orientation of the observer relative to the AGN axis [Urry and Padovani, 1995, Netzer, 2015, Hickox and Alexander, 2018]. Because the overall structure of an AGN is approximately axisymmetric, its appearance changes substantially with viewing angle. Objects that share the same underlying physical structure may therefore exhibit very different observational characteristics, leading them to be classified into distinct AGN types. The unified model of AGN provides a framework for interpreting this diversity by proposing that these different classes do not represent fundamentally different kinds of objects, but rather the same phenomenon observed from different perspectives. This unification is a crucial step toward identifying which intrinsic properties—such as black hole mass, spin, accretion rate, host galaxy characteristics, and environmental interactions—play the dominant role in shaping accretion processes, jet production, and radiation output [Urry and Padovani, 1995, Heckman and Best, 2014, Netzer, 2015].

2.2.4 Broad-Line Region and Emission Lines

The broad-line region (BLR) is a dense, inner region of an active galactic nucleus located approximately 10^{15} m from the central engine [Carroll and Ostlie, 2017], composed of ionised gas that produces the characteristic broad emission lines

observed in AGN spectra. These lines are broadened by large gas velocities that are gravitationally dominated, indicating that the BLR gas is moving primarily under the influence of the central supermassive black hole [Gaskell, 2009]. The BLR forms a thick, flattened structure that is closely linked to the surrounding dusty torus. It intercepts a large amount of the radiation from the central source, but because of its shape, type 1 AGN are usually observed from above the plane, which explains why strong absorption of ionising radiation is not seen. Radiation mainly escapes along the polar directions, while gas closer to the mid-plane is more shielded. As a result, gas closer to the black hole produces higher-ionisation emission lines, while lower-ionisation lines form farther out, up to the region where the dusty torus begins Gaskell [2009]. Physically, the BLR represents material in the process of accreting toward the black hole. The inferred inflow rate of the BLR gas is sufficient to supply the accretion needed to power the AGN. Because its motions are gravitationally dominated and its structure is broadly similar across AGN, the BLR provides a reliable basis for estimating supermassive black hole masses [Gaskell, 2009].

Broad emission lines in AGN spectra are produced by photoionisation from the continuum radiation. Broad lines such as Hα and Hβ vary on timescales of weeks to months [Carroll and Ostlie, 2017]. Hα in particular is an optical broad emission line produced by gas in the BLR whose width reflects the kinematics of this gas and is therefore used as a virial estimator of the black hole mass [Rakić, 2022] (see Section 4.1.2).

2.2.5 SMBH Mass Measurements from AGN

A central challenge in studying SMBH–galaxy co-evolution comes from observational biases in black hole mass measurements. Dynamical measurements require resolving the region where the black hole's gravity dominates, which is only possible in nearby galaxies and tends to favour systems with large stellar velocity dispersions and more massive black holes. In contrast, black hole masses derived from AGN spectra do not rely on resolving these small spatial scales. Instead, they use the widths of broad emission-line dispersions to estimate the black hole mass, allowing measurements for a much wider range of galaxies. For this reason, AGN samples are often considered less affected by the selection biases that influence dynamical measurements, although they remain biased toward actively accreting, unobscured black holes with measurable broad emission lines. Although stellar velocity dispersion is often considered a fundamental quantity in SMBH scaling relations, it depends strongly on how it is measured, whereas

black hole mass more directly reflects the accumulated growth of the black hole [Merritt and Ferrarese, 2001]. Many studies find that AGN-hosting galaxies lie below the $M_{\rm BH}$–$M_\star$ relation defined by inactive galaxies with dynamically measured black holes, in line with theoretical models in which feedback during active phases plays an important role in shaping the link between black holes and their host galaxies [Shankar et al., 2020].

2.2.6 Accretion Discs, Accretion Rate, and Radiative Output

Accretion onto a black hole occurs through a disc when the infalling gas carries angular momentum, requiring outward transport of angular momentum for matter to spiral inward. As material moves to smaller radii, gravitational potential energy is released and partially converted into radiation emitted from the disc [Shakura and Sunyaev, 1973].

The radiative output of the accretion disc depends primarily on the mass accretion rate, $\dot{M}$, which therefore represents the key parameter governing the luminosity of an accreting black hole. Under the assumption of radiatively efficient accretion, the total luminosity can be expressed as

$$L = \eta \dot{M} c^2, \tag{2.1}$$

where η is the radiative efficiency commonly adopted in AGN studies [Heckman and Best, 2014] and c is the speed of light. In thin accretion disc theory, η depends on the black hole spin and is approximately $\eta \simeq 0.06$ for a non-rotating (Schwarzschild) black hole, with higher values expected for rapidly rotating systems [Shakura and Sunyaev, 1973].

At high luminosities, radiation can interact with the surrounding gas, driving outflows and partially regulating further accretion. As a result, the bolometric luminosity is closely linked to the instantaneous accretion rate, while not necessarily reflecting the long-term growth history of the black hole [Shakura and Sunyaev, 1973].

2.2.7 Bolometric Luminosity as a Tracer of Accretion Rate

To investigate whether large-scale galactic structures, such as stellar bars, influence AGN activity, we use the bolometric luminosity as an indirect tracer of the accretion rate onto the central supermassive black hole. As established

above, the bolometric luminosity reflects the rate at which gravitational energy is released through accretion and converted into radiation.

In a simplified Newtonian picture, the bolometric luminosity may also be expressed as

$$L \simeq \frac{GM\dot{M}}{2r}, \tag{2.2}$$

where G is the gravitational constant, M is the black hole mass, $\dot{M}$ is the mass accretion rate, and r represents the characteristic radius at which the gravitational potential energy is released. Although this expression does not capture the full complexity of relativistic accretion discs, it illustrates the direct dependence of luminosity on the accretion rate [Horvath, 2022].

A high bolometric luminosity therefore indicates that the supermassive black hole is currently accreting material at a high rate, while a low bolometric luminosity suggests a lower accretion rate or a temporary quiescent phase. For this reason, bolometric luminosity is widely used as an observational proxy for the instantaneous accretion activity of AGN, and forms the basis for our analysis of the relationship between bar strength and nuclear activity [Shakura and Sunyaev, 1973].

2.3 BH mass estimation - virial method

To estimate black hole masses, we focus on unobscured AGN, where broad emission lines are clearly visible. In this context, single-epoch refers to the use of a single observation taken at one point in time, rather than long-term monitoring of variability. The width of a broad emission line measures the velocity of gas orbiting the black hole, while the line or continuum luminosity provides an empirical estimate of the size of this region, calibrated using reverberation-mapped AGN [Greene and Ho, 2005]. Recent work has shown that black hole masses derived using this single-epoch approach remain robust even when based on photometric rather than spectroscopic measurements [Chaves-Montero et al., 2022]. This approach allows black hole masses to be derived consistently for large samples. In these systems, the broad-line region is gravitationally influenced by the central black hole, leading to Doppler-broadened emission lines whose widths are related to the black hole mass [Blandford and McKee, 1982, Ho, 1999, Wandel et al., 1999]. We estimate SMBH masses using the widely adopted single-epoch virial relation of [Greene and Ho, 2005], which is calibrated using reverberation mapping, a method that measures the delay between changes in the AGN light

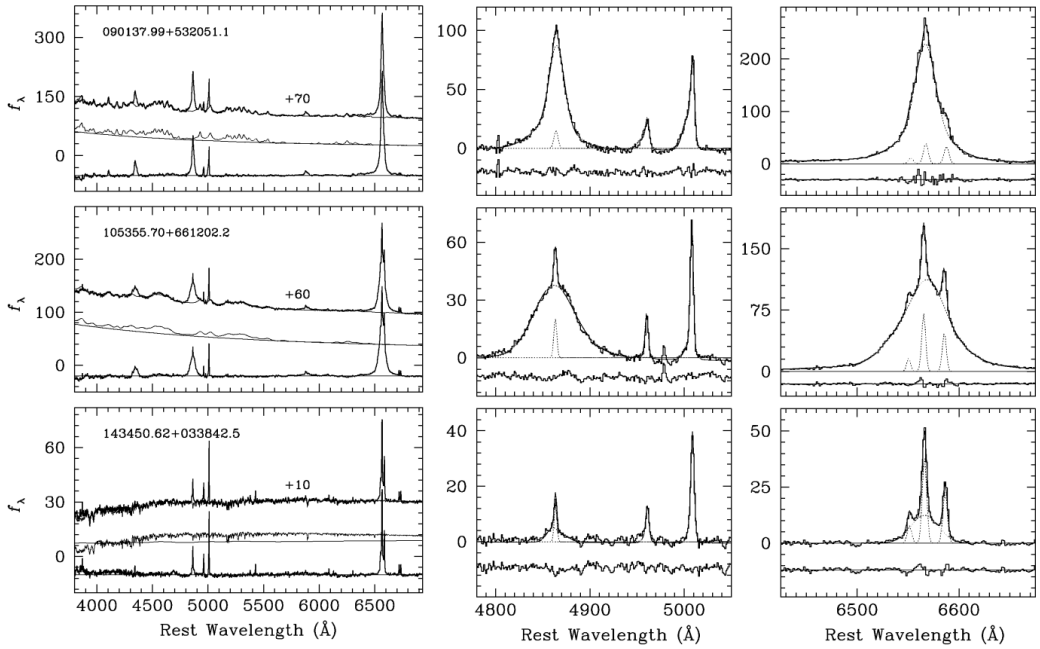

Figure 2.7: **Example single-epoch optical spectra of Type 1 AGNs from Greene and Ho [2005].** The left panels show the observed spectra with continuum models, the middle panels show fits to the Hβ+[O III] region, and the right panels show fits to the Hα+[N II] complex. The broad Hα component, whose width and luminosity are used to estimate black hole masses via the virial method, is clearly visible in all cases.

and the response of broad emission lines to estimate the black hole mass, [Kaspi et al., 2000, Peterson et al., 2004] and connects the black hole mass to the full width at half maximum (FWHM) and luminosity of the broad Hα emission line.

Greene and Ho [2005] developed a method for estimating SMBH masses using only the luminosity and line width of the broad Hα emission line (See Figure 2.7) in single-epoch AGN spectra. This method achieves uncertainties comparable to earlier approaches based on the optical continuum [Kaspi et al., 2000] defined as the optical continuum refers to the smooth infrared-to-ultraviolet emission of an AGN produced by non-stellar processes in the nuclear region [O'Dell, 1986], while avoiding difficulties that arise when the continuum is faint or strongly affected by host-galaxy light. Its reliability is based on two key empirical results. First, the luminosity of the broad Hα emission line closely follows the optical

continuum luminosity, showing that Hα traces the ionising radiation produced by the AGN. Second, the width of the Hα line strongly correlates with the widths of other broad Balmer lines, demonstrating that Hα provides a reliable measure of the gas velocities in the broad-line region [Kaspi et al., 2000]. Their large, homogeneous sample confirms that Hα reliably traces the virial velocities of BLR gas, and that broad Hα profiles are only marginally affected by radiative transfer effects or internal reddening. Because the Hα line is strong, observable across a wide luminosity range, and minimally influenced by host-galaxy starlight, the resulting Hα-based virial mass estimator offers a robust and practical tool for measuring black hole masses in unobscured AGNs where the broad-line region is directly visible [Greene and Ho, 2005].

Chapter 3

Data

3.1 Facilities Used

This work combines optical spectroscopic and high-resolution imaging data from multiple observatories, each contributing complementary information about active galaxies and their central black holes. The main datasets used are the Sloan Digital Sky Survey, the spectroscopy taken from Lick Observatory and the Hubble Space Telescope imaging.

3.1.1 SDSS

SDSS (Sloan Digital Sky Survey) originated in the late 1980s and early 1990s as part of the Astrophysical Research Consortium's effort to build a dedicated wide-field survey telescope at Apache Point Observatory (APO). Supported by the Alfred P. Sloan Foundation and developed through a collaboration including Princeton, IAS, Chicago, JHU, UW, and later several international partners, SDSS constructed a dedicated 2.5 m telescope engineered as an integrated imaging–spectroscopy system. The telescope provides a 3° field of view with stable image quality across the focal plane, enabling efficient drift-scan (time-delay-and-integrate) imaging in five optical filters (u, g, r, i, z) to a depth of $r \approx 23$ mag. These imaging data are used to select targets for spectroscopy with dual fibre-fed spectrographs, designed to obtain approximately one million galaxy and quasar redshifts over the planned five-year survey. Although originally expected to begin around 1995, survey operations began in April 2000 and ultimately produced a foundational data set for studies of large-scale structure and the broader extragalactic sky [Peterson and Mackie, 2006].

SDSS provides wide-field optical imaging and spectroscopy of galaxies across the northern sky, along with extensive stellar spectroscopy, and substantially larger samples expected in DR20 [Collaboration et al., 2025]. SDSS spectra are widely used to estimate SMBH masses through single-epoch (virial) methods, which rely on the width and luminosity of broad emission lines such as Hα and Hβ [Vestergaard and Peterson, 2006]. These measurements make SDSS a cornerstone for statistical studies of active galactic nuclei (AGN) [York et al., 2000]. In this thesis, SDSS imaging data from DR8 are used to define and select the DISKDOM galaxy sample, while the spectroscopic measurements required for black hole mass estimation are primarily provided by Lick Observatory, with SDSS spectra used only for a small number of galaxies lacking Lick observations [Simmons et al., 2017].

3.1.2 Shane/Kast at Lick

Lick follow-up spectroscopy was obtained by the Kast Double Spectrograph on the Shane 3 m Telescope at Lick Observatory. Kast is a dual-beam instrument mounted at the Cassegrain focus, consisting of two optimised spectrographs, one blue and one red, housed in a common structure. A diachroic beamsplitter and two independent CCD detectors enable simultaneous blue- and red-channel observations, while a range of gratings provides higher-quality data, with substantially improved signal-to-noise relative to the SDSS spectra of the same objects. This enables a more robust decomposition of broad and narrow emission-line components and yields more precise measurements of the line widths used in black hole mass determinations [Lick Observatory, 2024]. Consequently, Lick spectroscopy serves as a valuable complement to SDSS by enhancing the reliability of emission-line measurements for selected targets [Park et al., 2012]. The Lick spectra were reduced using standard procedures, including cleaning, wavelength calibration, and flux calibration. Emission-line fitting was performed to derive redshifts and AGN properties. To isolate host-galaxy features, the AGN contribution was removed using PSF (Point Spread Function) modelling, a commonly used technique to disentangle the bright unresolved nucleus from surrounding stellar light in both images and spectra.

3.1.3 Hubble Space Telescope (*HST*)

High-resolution ***HST*** imaging provides more robust morphological information than ground-based surveys, because atmospheric seeing blurs small-scale struc-

tures that *HST* can resolve. While ground-based data (e.g. SDSS or DESI) enable basic morphological classification, the *HST* data allow more reliable identification and measurement of structural features such as bars, bulges, and discs. Two-dimensional image decompositions performed on *HST* images provide accurate measurements of structural parameters including bulge-to-total ratios, axis ratios, Sérsic indices, and quantitative bar-strength metrics. These measurements allow us to characterise host-galaxy morphology at the scales relevant for secular evolution and to correlate these properties with black hole masses and AGN luminosities derived from the SDSS spectroscopy [e.g. Peng et al., 2002, Fahey et al., 2025].

3.2 Samples Used

3.2.1 DISKDOM Sample (Simmons et. al. 2017)

We use a sample originally introduced by Simmons et al. [2017], who presented a large and well-defined set of 101 luminous Type 1 AGN hosted in disc-dominated galaxies with no significant bulge component. The sample covers a broad range of stellar masses, reaching up to approximately $2 \times 10^{11}\, M_{\odot}$, and is uniquely suited for studying black hole (BH) growth in galaxies evolving through merger-free, or secular, processes.

The AGN in the DISKDOM sample were selected from the W2R catalogue, which contains 4316 high-confidence, unobscured AGN candidates Simmons et al. [2017]. The catalogue is based on a multi-wavelength photometric selection combining:

- WISE (Wide-field Infrared Survey Explorer) infrared colours,
- 2MASS (Two Micron All-Sky Survey) near-infrared measurements,
- RASS (ROSAT All-Sky Survey) X-ray detections.

This approach identifies unobscured AGN with a confidence level exceeding 95%. It is particularly suitable for studies requiring broad emission lines, which are essential for accurate virial BH mass estimates Simmons et al. [2017].

The W2R AGN sample was cross-matched with SDSS Data Release 8 yielding 1844 sources located within $3''$ of SDSS imaging. Morphological classification was then performed manually through visual inspection of SDSS colour images. From this process, 137 galaxies were selected based on the presence of clear disc features (e.g. spiral arms, bars) or the absence of a visible bulge.

The SDSS-matched subsample spans a low-redshift range, meaning that the galaxies are nearby and well resolved. This enables detailed investigation of secular (non-merger) evolutionary processes in the present-day Universe.

In their study, the authors used the width of the broad Hα emission line as a virial indicator to estimate BH masses. These masses were then compared with two host-galaxy properties: the total stellar mass and cautious upper limits on bulge stellar mass, acknowledging the inherent difficulty of measuring bulge components in galaxies hosting bright AGN.

The parent sample consists of 137 disc-dominated AGN identified through SDSS imaging. From this, a subset of 101 galaxies was defined based on the availability of spectroscopic data, comprising 96 galaxies that already had available spectra from SDSS, primarily from Data Release 9 (DR9), which incorporates earlier data, including that from DR7. For five additional galaxies, spectra were obtained using the Intermediate Dispersion Spectrograph (IDS) on the Isaac Newton Telescope (INT) in May 2014. These observations targeted the Hα region, which is essential for BH mass estimation.

All spectra were reduced using standard pipelines, and each of the 101 galaxies in the final sample displays a broad Hα emission line, confirming their classification as unobscured Type 1 AGN Simmons et al. [2017].

Thus, the final DISKDOM sample consists of 101 broad-line AGN hosted in disc-dominated galaxies at relatively low redshift. Their proximity allows for a detailed analysis of both morphological structure and spectral properties.

3.2.2 Lick Sample (Garland et al. 2023)

The data set analysed by Garland et al. [2023] is built directly on the DISKDOM parent sample introduced by [Simmons et al., 2017], described in the preceding section. This original sample consists of 137 disc-dominated AGN host galaxies selected through multi-wavelength photometric data (the W2R catalogue) and visual morphological classification from SDSS imaging.

[Garland et al., 2023] obtained new spectroscopic observations for a subset of these galaxies using the Lick Observatory, with the aim of investigating off-nuclear star formation and structural properties in disc-dominated AGN hosts.

In total, 56 galaxies were observed at Lick, 21 of which also have SDSS spectra. Four galaxies lacked any spectral coverage and were excluded from further analysis. Their final *AGNDISCS* sample therefore consists of 56 disc-dominated Type 1 AGN with Lick spectroscopy.

3.2.3 HST Sample (Fahey et al. 2025)

While the previous section focused on the spectroscopic follow-up of disc-dominated AGN using SDSS and Lick data, this section presents the high-resolution imaging analysis performed with *HST*. *HST* provides the spatial resolution necessary for precise structural decomposition, allowing the different morphological components of each galaxy to be reliably separated and quantified.

The 100 galaxies observed with *HST* and analysed by Fahey et al. [2025] were drawn from the SDSS imaging-selected parent sample of 137 disc-dominated AGN described above: unobscured Type 1 AGN hosted in disc-dominated galaxies with little or no bulge contribution. These properties make the sample ideal for studying structural evolution in galaxies thought to be evolving primarily through secular, merger-free processes.

Each galaxy was modelled using `GALFIT`, a two-dimensional surface-brightness fitting tool widely used in extragalactic astronomy. `GALFIT` fits user-specified analytic light profiles (e.g., Sérsic functions) directly to the imaging data. The decomposition therefore depends on physically motivated model choices, and the resulting parameters must be interpreted by the user to separate contributions from the disc, bulge, bar, and unresolved AGN nucleus [Peng et al., 2002, 2010].

Once the final models were constructed, each fitted component was assigned a morphological classification by an expert classifier. The classification relied primarily on parameters derived from the Sérsic model:

- **Disc components:** characterised by a large effective radius and a low Sérsic index
- **Bulges or central concentrations:** compact components with high Sérsic index, indicating strong central light concentration.
- **Bars:** identified through the presence of truncation functions in the `GALFIT` model, which reproduce the flat-topped, elongated light profile typical of stellar bars.
- **Spiral arms:** identified by the presence of non-axisymmetric spiral components in the model, specifically via the inclusion of spiral inner and outer radius parameters [Fahey et al., 2025].

A small number of galaxies were excluded after modelling due to clearly elliptical morphology, as these do not match the disc-dominated selection criteria of the parent sample. The final HST-imaged sample therefore contains 92 well-modelled AGN host galaxies.

This HST-based structural analysis provides the most accurate measurement of the luminosity distribution among the different components (disc, bar, bulge, and AGN) in these merger-free AGN host galaxies available for this thesis.

3.2.4 Final Sample Selection

From the SDSS imaging-selected parent sample of 137 galaxies, a spectroscopic DISKDOM sample of 101 galaxies was defined. From the spectroscopic DISKDOM sample, only systems exhibiting a clearly identifiable stellar bar were selected for further analysis. The resulting barred-galaxy subsample consists of 23 objects.

To summarise the overlap between the different datasets, 75 galaxies have spectroscopic data only from SDSS, 35 only from Lick Observatory, and 21 from both facilities, with an additional five galaxies observed using the INT and one galaxy lacking usable spectroscopy. High-resolution *HST* imaging is available for 92 galaxies in total and provides the structural information required to measure bar properties for those systems included in the barred-galaxy subsample.

Bolometric luminosities were available for all 23 barred galaxies and were therefore used for the analysis of the relationship between bar strength and bolometric luminosity.

The determination of black hole masses was less uniform across the sample. For a subset of the barred galaxies, black hole masses were adopted from Lick Observatory measurements. For barred galaxies lacking Lick-based mass estimates but having available SDSS spectra (g002, g006, g020, g106), black hole masses were derived using data from SDSS.

For one barred galaxy (g121), neither Lick measurements nor SDSS spectra were available, preventing a reliable estimation of the black hole mass. As a result, the analysis of black hole mass versus bar strength is based on 22 galaxies rather than the full barred sample of 23 objects. Representative *HST* cutout images of all barred galaxies in the final sample are shown in the Figure 3.1.

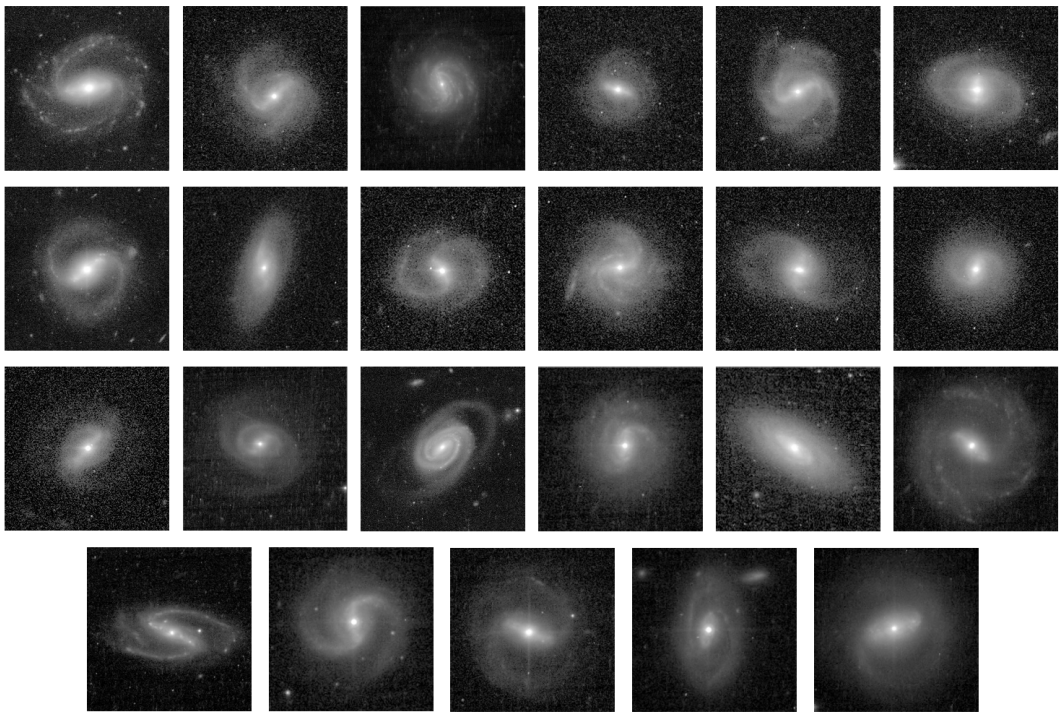

Figure 3.1: HST images of barred galaxies in the final sample. Images are ordered by increasing right ascension. First row (left to right): g029, g037, g038, g039, g048, g060. Second row (left to right): g068, g072, g073, g084, g085, g086. Third row (left to right): g087, g098, g101, g103, g109, g116. Fourth row (left to right): g002, g006, g020, g106, g121. North is up and east is to the left.

Chapter 4

Methodology

4.1 Calculation Analysis

4.1.1 Derivation of Emission-Line and Structural Parameters

For each available galaxy, we used the broad Hα velocity dispersions reported by Garland et al. [2023]. These dispersions, $\sigma_{\mathrm{H}\alpha,\mathrm{broad}}$ (in $\mathrm{km\,s^{-1}}$), together with their associated uncertainties, were converted to full width at half maximum (FWHM) values for use in the black hole mass calculation. The conversion from dispersion to FWHM was performed using

$$\mathrm{FWHM} = 2.355\,\sigma. \tag{4.1}$$

We computed the total broad-line flux by combining the fitted amplitude of the broad Hα component with the line width,

$$F_{\mathrm{H}\alpha} = \sqrt{2\pi}\,A\,\Delta\lambda, \tag{4.2}$$

where A is the Gaussian amplitude and $\Delta\lambda$ is the Gaussian dispersion of the broad component.

We then computed its luminosity fraction relative to the host. For each structural component i,

$$L_{\mathrm{frac},i} = \frac{L_i}{L_{\mathrm{host}}}. \tag{4.3}$$

Host luminosity uncertainties were estimated as

$$\delta_{L_{\rm host}} = \frac{1}{2}\left(L_{\rm host,max} - L_{\rm host,min}\right), \tag{4.4}$$

where $L_{\rm host,max}$ and $L_{\rm host,min}$ are the maximum and minimum host luminosities permitted by the modelling.

We then cross-matched the Lick emission-line catalogue with the *HST* structural catalogue (nearest-neighbour match with a search radius of $3''$), and computed luminosity distances $D_{\rm L}(z)$, which were used to convert Hα fluxes to luminosities,

$$L_{\rm H\alpha} = 4\pi D_{\rm L}^2 F_{\rm H\alpha}. \tag{4.5}$$

4.1.2 Black Hole Mass Estimation

The mass of the central black hole was estimated using a single-epoch virial method based on the broad Hα emission line. This technique relies on the empirical correlation between the size of the broad-line region (BLR) and the AGN continuum luminosity, established through reverberation-mapping studies. [Greene and Ho, 2005] recalibrated this radius–luminosity relation using updated lag measurements from [Peterson et al., 2004], applying a consistent cosmology and retaining only the most reliable data. Their fit gives a BLR size scaling as

$$R_{\rm BLR} \propto L_{5100}^{0.64}, \tag{4.6}$$

which, when combined with the virial assumption for BLR gas dynamics, leads to a mass relation of the form $M_{\rm BH} \propto R_{\rm BLR}\,{\rm FWHM}^2$.

Because the continuum luminosity and the Hα properties are tightly correlated, this expression can be fully rewritten in terms of the Hα line alone. Substituting the relevant empirical relations into the virial formula yields the widely used Hα-based estimator:

$$M_{\rm BH} = (2.0^{+0.4}_{-0.3}) \times 10^6 \left(\frac{L_{\rm H\alpha}}{10^{42}\,{\rm erg\,s^{-1}}}\right)^{0.55} \left(\frac{{\rm FWHM_{H\alpha}}}{10^3\,{\rm km\,s^{-1}}}\right)^{2.06} M_\odot. \tag{4.7}$$

In practice, this method offers several advantages: the Hα line is typically stronger and less affected by host-galaxy contamination or dust extinction, and all required quantities can be extracted from a single optical spectrum. For the galaxies in our matched sample, black hole masses were computed using this calibrated Hα virial estimator [Greene and Ho, 2005].

4.1.3 Bar identification and bar-strength measurement

For each `GALFIT` component identified as a bar, we used its axis ratio q, luminosity L_i, and luminosity fraction $L_{\mathrm{frac},i}$. The bar-strength parameter for a given component was defined as

$$\phi_i = (1 - q_i)\, L_{\mathrm{frac},i} \tag{4.8}$$

where the axis ratio q (ranging from 0 to 1) describes the elongation of each component, $L_{\mathrm{frac},i}$ denotes its fractional luminosity, and ϕ_i is the bar-strength measure [Weinzirl et al., 2009].

This metric captures how elongated a component is and how bright it is compared to the rest of the source — a strong bar will have both high ellipticity (low axis ratio) and high light contribution (for example, high L_{frac} and low q indicating a strong bar, very round and faint components indicating no bar).

4.2 Comparison Between SDSS and Lick-Derived Black Hole Masses

To assess the consistency between black hole mass estimates derived from different spectroscopic sources, we compared values obtained from SDSS spectra and those derived from Lick spectra. This comparison was performed for the 17 galaxies with both measurements available. Figure 4.1 presents a scatter plot with SDSS-based black hole masses on the x-axis and Lick-based masses on the y-axis. Each point represents a galaxy observed with both instruments. A reference line is included to indicate where perfect agreement would lie.

The scatter plot shows that most points lie below the identity line, indicating that SDSS-based black hole masses are generally higher than those derived from our Hα analysis

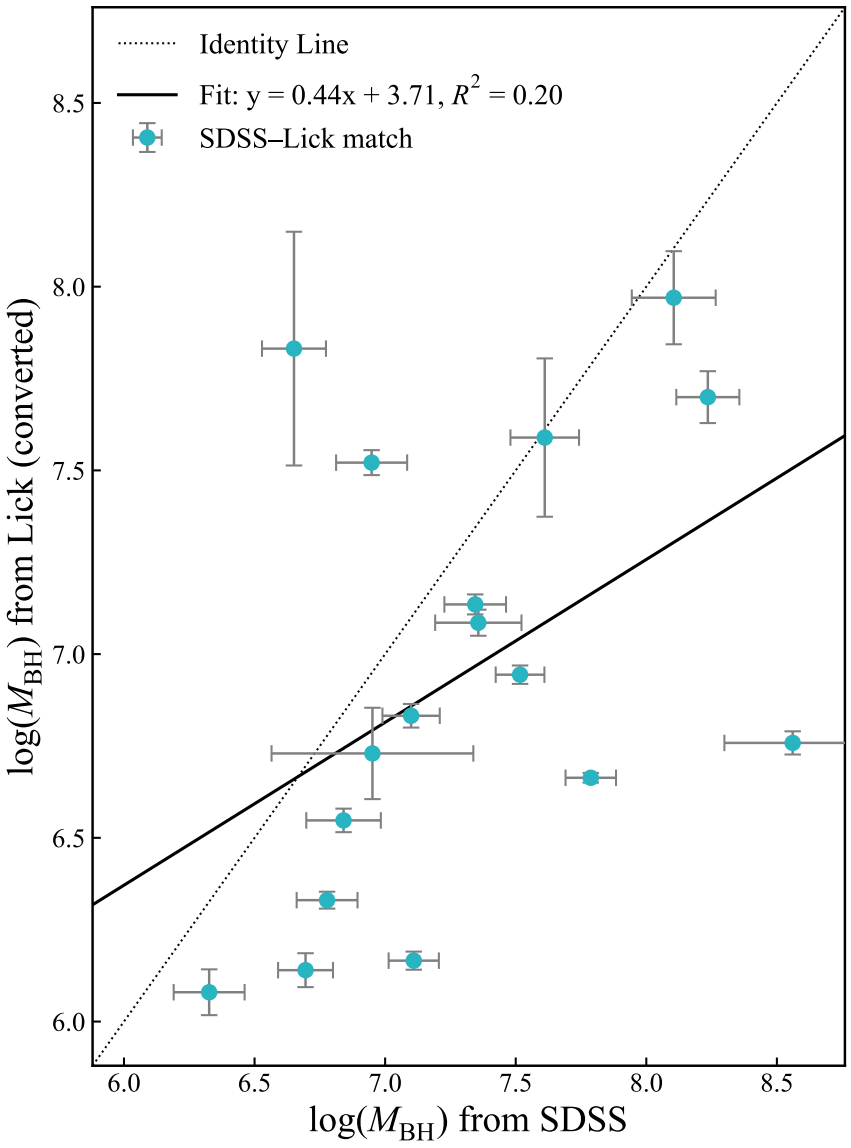

Figure 4.1: **SDSS vs. Lick-Derived Black Hole Masses**. The figure shows a comparison between black hole masses derived from SDSS spectra and those derived from Lick Observatory data for galaxies with measurements available from both sources. Black hole masses are expressed as $\log(M_{\rm BH}/M_{\odot})$. SDSS-based black hole masses are shown on the x-axis, while Lick-derived masses are shown on the y-axis. Each point represents an individual galaxy observed with both instruments. The dashed diagonal line indicates the identity relation, where both mass estimates would be equal, while the solid line shows a linear fit to the data.

Chapter 5

Results

This section presents the results of the analysis of the relationship between stellar bar strength and two properties of active galactic nuclei: the mass of the central supermassive black hole and the bolometric luminosity. These two quantities probe different aspects of black hole growth, with the black hole mass reflecting the long-term evolutionary history and the bolometric luminosity tracing the current accretion activity.

The results are presented in two subsections. First, the dependence of black hole mass on bar strength is examined in order to test whether the presence or strength of a stellar bar is linked to the final mass of the central black hole. Second, the relationship between bar strength and bolometric luminosity is analysed to investigate a possible connection between bars and ongoing AGN fuelling. In both cases, the analysis combines visual inspection of the data with statistical correlation tests to quantify the strength and significance of any observed trends.

5.1 Black Hole Mass vs. Bar Strength

Figure 5.1 shows the relationship between bar strength (ϕ_{bar}) and the mass of the central supermassive black hole. The analysis includes 22 barred galaxies, as one object lacks a reliable black hole mass estimate (see Section 3.2.4). 51 unbarred galaxies are included, displayed as a vertical distribution at $\phi_{\mathrm{bar}} = 0$.

Visually, the plot does not reveal a clear trend between bar strength and black hole mass. This impression is supported by statistical analysis, summarised in Table 5.1.

Both the visual inspection and the statistical results indicate that no significant linear or monotonic correlation between bar strength and black hole mass

Table 5.1: Correlation results between Bar Strength and Black Hole Mass.

Statistic	**Value**	**Significance**
Pearson correlation (r)	-0.036	$p = 8.730e-01$ (not significant)
Spearman correlation (ρ)	-0.083	$p = 7.134e-01$ (not significant)

is present in this sample.

In order to assess whether the mere presence of a stellar bar has a measurable impact on the masses of supermassive black holes, we compared the black hole mass distributions of barred and unbarred galaxies. We constructed normalised histograms of the logarithm of the black hole mass, $\log(M_{\rm BH}/M_{\odot})$, for the two populations.

The resulting histograms (Figure 5.1) show a substantial overlap between the barred and unbarred samples across the full mass range probed. Both distributions peak at similar values, around $\log(M_{\rm BH}/M_{\odot}) \sim 7.3$–$7.6$, and exhibit comparable widths. No clear systematic shift toward higher or lower black hole masses is observed for either population. Although minor differences appear at the high-mass end, these are small and do not indicate a distinct separation between the two distributions.

In order to quantitatively evaluate whether the observed differences are statistically significant, we performed a two-sample Kolmogorov–Smirnov (KS) test on the barred and unbarred samples. We can see the results in Table 5.1. The high p-value indicates that the null hypothesis, namely that the two samples are drawn from the same parent distribution, cannot be rejected.

Table 5.2: Kolmogorov–Smirnov test comparing black hole mass distributions of barred and unbarred galaxies.

Statistic	**Value**
KS statistic (D)	0.159
p-value (p)	0.73

These results suggest that, in this sample, the presence of a stellar bar alone does not lead to a statistically significant difference in black hole mass. This finding implies that bars are not a dominant driver of long-term black hole growth, and that other factors, such as gas availability, bulge properties, or accretion history, likely play a more important role in regulating supermassive black hole mass.

5.2 Bar Strength vs. Bolometric Luminosity

We examine the relationship between bolometric luminosity and bar strength in order to investigate whether the presence and strength of a stellar bar are connected to the efficiency of AGN fuelling.

Figure 5.3 shows the dependence of the bolometric luminosity on the strength of the bar. A moderate negative trend is visible, suggesting that galaxies with stronger bars tend to host less luminous AGN within this sample.

Table 5.3: Correlation results between Bar Strength and Bolometric Luminosity.

Statistic	**Value**	**Significance**
Pearson correlation (r)	-0.48	$p = 0.020$ (**significant**)
Spearman correlation (ρ)	-0.32	$p = 0.136$ (not significant)

This visual impression is supported by a statistical analysis summarised in Table 5.2. The Pearson correlation coefficient yields a value of $r = -0.48$ with a significance level of $p = 0.020$, indicating a statistically significant negative correlation. In contrast, the Spearman rank correlation coefficient ($\rho = -0.32$, $p = 0.136$) is not statistically significant, implying that the monotonicity of the relation is weaker and sensitive to outliers.

These results suggest that stronger bars are associated with lower bolometric luminosities in AGN host galaxies, although the strength of this relation depends on the adopted statistical measure and the limited size of the sample.

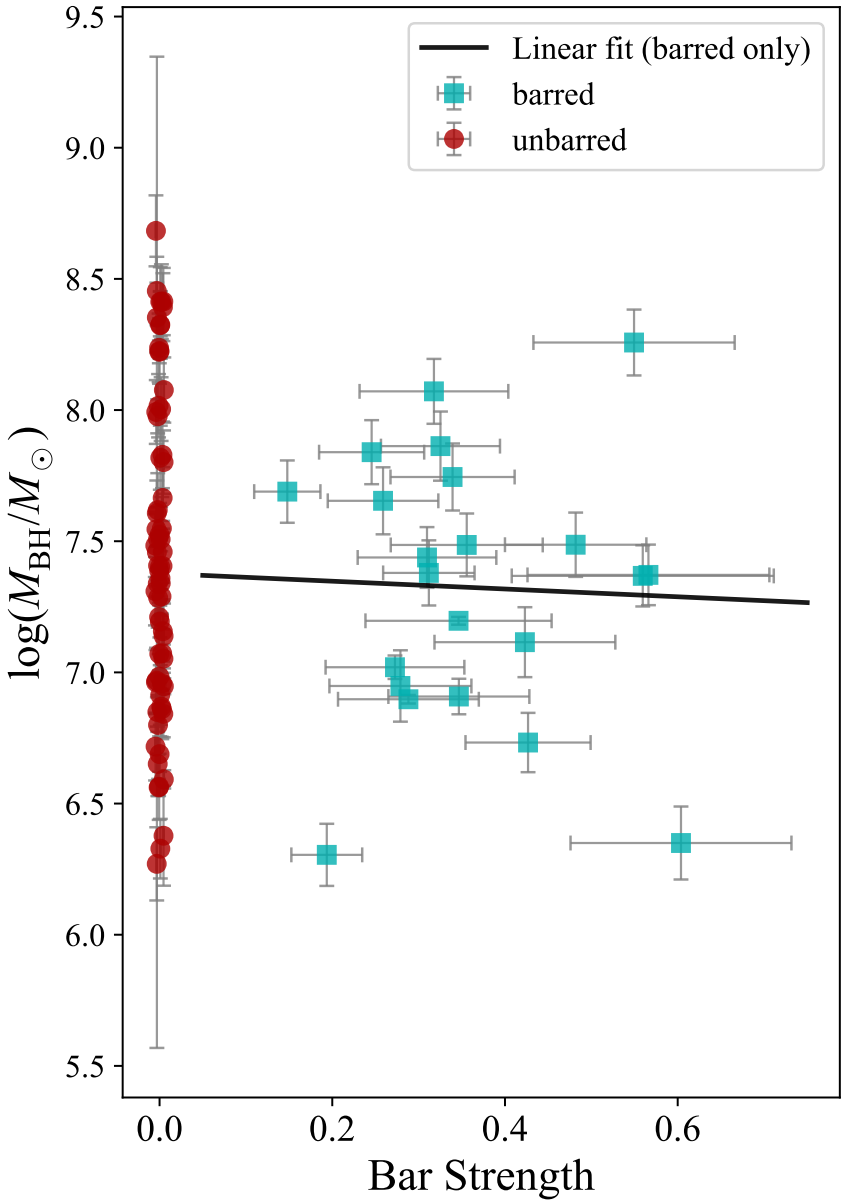

Figure 5.1: **Bar Strength vs Black Hole Mass**. The figure shows how black hole mass changes with bar strength across the full galaxy sample. Bar strength is shown on the x-axis, while the logarithm of the black hole mass is shown on the y-axis. Unbarred galaxies are concentrated near zero bar strength, whereas barred galaxies extend to higher bar strength values. A straight line is fitted only to the barred galaxies and is shown as a solid line.

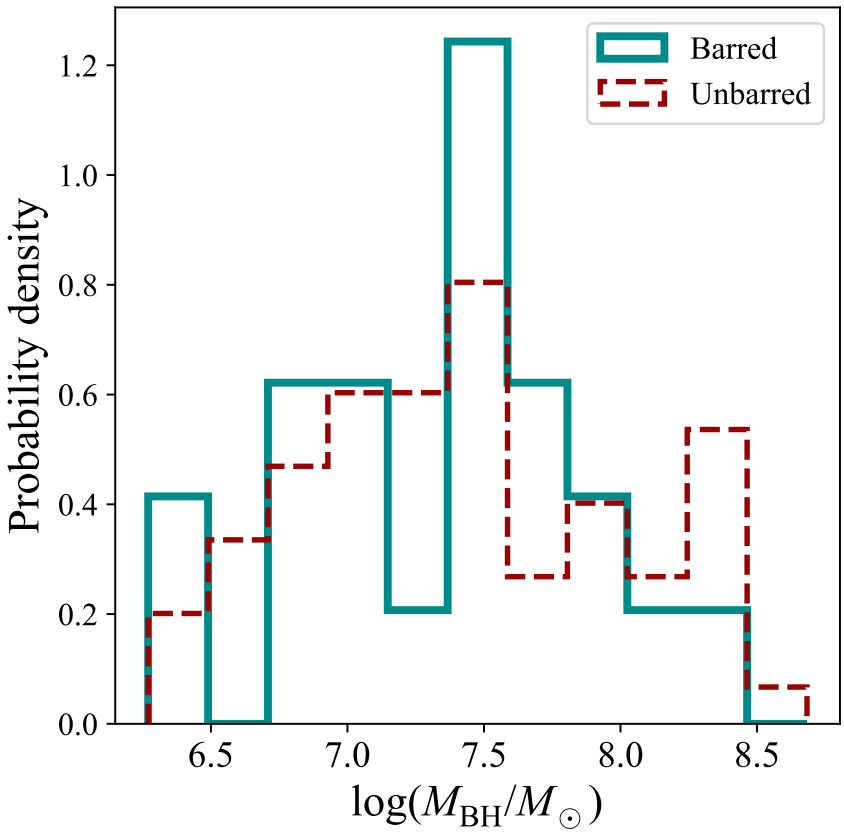

Figure 5.2: **Black hole mass distributions in barred and unbarred galaxies**. The figure compares the distributions of black hole masses in barred and unbarred galaxies using normalised histograms of $\log(M_{\rm BH}/M_{\odot})$. The two populations exhibit substantial overlap across the full mass range probed, with both distributions peaking at similar values around $\log(M_{\rm BH}/M_{\odot}) \sim 7.3$–$7.6$. No clear systematic shift toward higher or lower black hole masses is observed for either barred or unbarred systems.

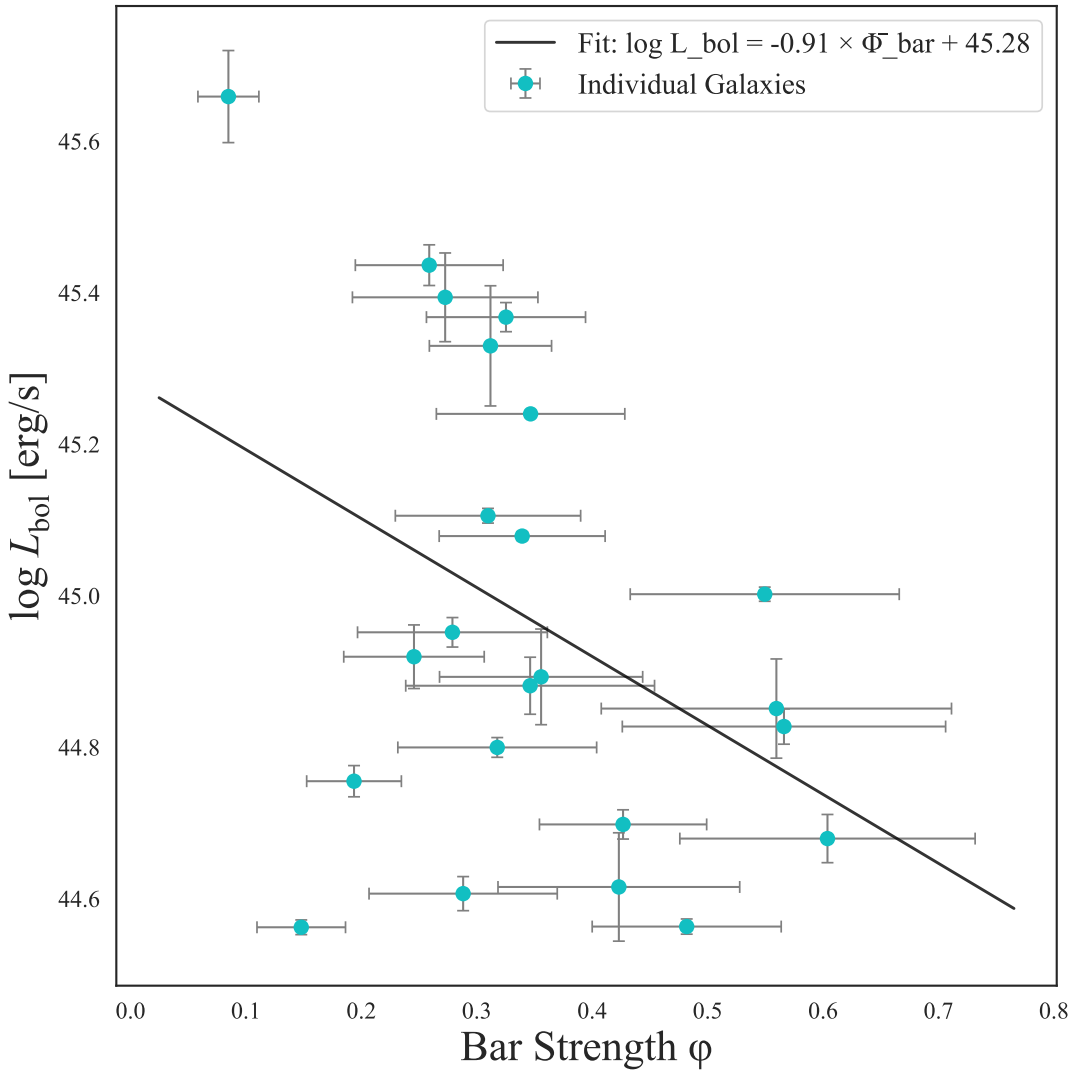

Figure 5.3: **Bar Strength vs. Bolometric Luminosity**. The logarithm of the AGN bolometric luminosity, $\log(L_{\rm bol}/{\rm erg\,s^{-1}})$, is shown as a function of the bar strength parameter ϕ for galaxies hosting stellar bars. The solid black line shows the best-fitting linear regression to the data. The fitted relation reveals a negative slope, indicating that galaxies with stronger bars tend to host AGN with lower bolometric luminosities, although with substantial scatter.

Chapter 6

Discussion

This work finds no significant relationship between stellar bar strength and the mass of the central supermassive black hole, while revealing a moderate negative correlation between bar strength and AGN bolometric luminosity. In addition, the black hole mass distributions of barred and unbarred galaxies are statistically indistinguishable, indicating that the mere presence of a bar does not lead to systematically different black hole masses. These findings indicate that stellar bars do not play a dominant role in driving the long-term growth of supermassive black holes, as reflected in black hole mass. However, the observed decrease in bolometric luminosity with increasing bar strength indicates that galaxies hosting stronger bars tend to host less luminous, and therefore less actively accreting AGN at the present epoch. This implies that while bars may influence the short-term accretion state of the AGN, their role in regulating sustained black hole growth is likely secondary to other factors such as gas availability, accretion history, or host-galaxy properties.

Recent large-sample studies suggest that strong and weak bars are not fundamentally different structures, but instead represent a continuous range of bar properties. Using Galaxy Zoo DECaLS (a volunteer-based visual morphological classification of galaxies) Géron et al. [2021] showed that many of the apparent differences between strong and weak bars largely disappear once bar length is taken into account, supporting earlier work arguing for a smooth distribution of bar strengths [de Vaucouleurs, 1959, Elmegreen and Elmegreen, 1985, Athanassoula, 2003]. In this context, treating bar strength as a continuous parameter, as done in this work, provides a natural way to test whether AGN properties change gradually with bar strength rather than abruptly between bar classes. The lack of a correlation between bar strength and black hole mass in our sam-

ple is therefore consistent with a scenario in which bar-driven secular processes do not directly control long-term black hole growth.

At the same time, recent studies show that bar strength is closely linked to how often galaxies host AGN. Using a large Galaxy Zoo DESI (a volunteer-based morphological classification of galaxies combined with data from the Dark Energy Spectroscopic Instrument) sample, Garland [2024] found that the fraction of optically selected AGN increases steadily from unbarred to weakly barred and strongly barred disc galaxies, even after accounting for differences in stellar mass and colour. In particular, strongly barred galaxies were found to be more than twice as likely to host an AGN as unbarred systems. These results suggest that while bars are not required for a galaxy to grow a supermassive black hole, they significantly increase the likelihood that nuclear activity is triggered, and that bar strength remains a meaningful parameter despite forming a continuum [Garland, 2024].

However, a higher likelihood of hosting an AGN does not necessarily imply a higher level of AGN power. Observational studies have shown that strong bars are more common in quiescent, gas-poor galaxies and are associated with lower gas reservoirs and shorter gas depletion timescales [Masters et al., 2012, Fraser-McKelvie et al., 2020]. Recent work has also shown that barred galaxies can host relatively strong nuclear activity while still exhibiting slightly lower black hole masses, indicating that bars may primarily influence how efficiently gas is accreted rather than how much mass the black hole gains overall [Marels et al., 2025]. Although bars can drive gas toward the central regions, they can also trap gas in resonances or redistribute it into ring-like structures, limiting sustained inflow [Buta, 1987, Kormendy and Kennicutt, 2004, Athanassoula, 1992]. Within this framework, the observed trend toward lower bolometric luminosities at higher bar strengths in our sample can be understood as AGN that are triggered more frequently in strongly barred galaxies, but are accreting less efficiently at the present epoch. This reconciles the higher AGN incidence reported by Garland [2024] with the absence of a corresponding increase in black hole mass.

Several observational studies have found little or no evidence for a direct link between large-scale bars and AGN activity. Using X-ray–selected AGN from multiple surveys, Cheung et al. [2013] found that AGN host galaxies are no more likely to host bars than comparable inactive galaxies. They also found no significant difference in the AGN fraction between barred and unbarred disc galaxies, leading them to conclude that large-scale bars are unlikely to be a primary fuelling mechanism for moderate-luminosity AGN at these epochs. Similar results

have been reported in the local Universe, where several studies find no excess of bars in active galaxies and no clear correlation between bar presence and AGN power [e.g., Ho et al., 1997, Mulchaey and Regan, 1997, Martini and Pogge, 1999, Erwin and Sparke, 2002, Lee et al., 2012].

These findings are not inconsistent with the results of this work. While Cheung et al. [2013] investigate whether bars increase the likelihood of hosting an AGN by comparing active and inactive galaxies, the present study instead focuses on how AGN properties vary with bar strength within an AGN-selected sample [Cheung et al., 2013]. In addition, differences in redshift range, AGN selection, and the use of discrete bar classifications rather than continuous bar-strength measures likely contribute to the differing conclusions. These studies suggest that the impact of bars on AGN fuelling depends strongly on the sample, methodology, and the specific aspect of AGN activity being examined.

Several limitations should be considered when interpreting these results. First, the final barred-galaxy subsample is small: out of the 101 galaxies in the parent sample, only 23 host a clearly identifiable stellar bar, and reliable black hole mass estimates are available for 22 of these systems. This limited sample size reduces the statistical power of the analysis and makes the results more sensitive to scatter and individual objects.

Second, the sample is restricted to unobscured Type 1 AGN. As a result, this study does not measure how frequently AGN occur as a function of bar strength, but instead focuses on how AGN properties vary once nuclear activity is already present. The results therefore probe black hole mass and instantaneous accretion activity within an AGN-selected population, rather than AGN triggering itself.

Finally, black hole masses estimated from the broad Hα emission line carry intrinsic uncertainties, and bolometric luminosities trace the instantaneous accretion state of the AGN, which may be affected by variability. In addition, the bar-strength measurements rely on structural modelling and are subject to uncertainties associated with the decomposition process. Despite these limitations, the results are consistent with recent large-sample studies and are robust within the scope of the available data.

Chapter 7

Conclusion

In this thesis, we investigated whether large-scale stellar bars influence the growth and activity of supermassive black holes in disc-dominated, merger-free galaxies hosting unobscured active galactic nuclei. By combining spectroscopic measurements from SDSS and Lick Observatory with high-resolution *HST* imaging, we analysed a carefully selected sample designed to isolate secular evolutionary processes from merger-driven effects.

Two complementary indicators of black hole growth were examined. Black hole mass was used as a tracer of long-term, integrated growth, while bolometric luminosity was adopted as a proxy for the current accretion rate onto the black hole [Shakura and Sunyaev, 1973, Horvath, 2022]. This approach allowed us to distinguish between processes affecting cumulative mass assembly and those influencing instantaneous accretion activity.

No evidence was found for a systematic relationship between stellar bar strength and black hole mass. Both correlation analyses and comparisons between barred and unbarred systems indicate that the presence or strength of a bar does not lead to a measurable difference in the final mass of the central black hole within this sample. This suggests that stellar bars are not a dominant factor governing long-term black hole growth in disc-dominated galaxies.

In contrast, a moderate negative trend is observed between bar strength and AGN bolometric luminosity, although with substantial scatter and sensitivity to the adopted statistical measure. Interpreted conservatively, this result points to a possible connection between bar strength and the current accretion state of the black hole, rather than its accumulated mass. Since bolometric luminosity traces the rate at which gravitational energy is released through accretion, this behaviour is consistent with a scenario in which bars influence the timing or

efficiency of gas inflow without determining the total amount of mass ultimately accreted.

Together, these findings support a picture in which stellar bars primarily modulate short-term accretion activity rather than driving sustained black hole growth. While bars are expected to redistribute angular momentum and transport gas toward central regions through secular processes [Sellwood and Wilkinson, 1993, Kormendy and Kennicutt, 2004], additional mechanisms are likely required to regulate gas inflow on the smallest scales and to control the long-term evolution of supermassive black holes in merger-free galaxies.

7.1 Future work

Observations of cold molecular gas provide strong evidence that stellar bars are efficient at redistributing gas within galaxies. CO surveys of nearby spirals show that barred galaxies typically have a higher concentration of molecular gas in their central kiloparsec than unbarred systems, supporting the idea that bars drive gas inward through gravitational torques [Sakamoto et al., 1999, Sheth et al., 2005]. However, these same studies also reveal important complexity. A significant fraction of early-type barred galaxies show little or no molecular gas in their central regions, suggesting that the bar has already transported gas inward and that this gas has subsequently been consumed by star formation [Sheth et al., 2005]. This implies that bar-driven inflow is likely a time-dependent process, with bars being most effective during a limited evolutionary phase. Importantly, the presence of gas in the central regions does not by itself imply ongoing inflow, making it necessary to distinguish between gas accumulation and active gas transport.

Optical data alone cannot fully capture this picture. As emphasised by Hickox and Alexander [2018], dust and gas obscure key stages of AGN fuelling and star formation, with dust dominating absorption at UV–optical wavelengths and gas playing a major role at X-ray energies. Mid-infrared observations are therefore essential for tracing obscured star formation and buried AGN activity, while millimetre and submillimetre observations directly probe the cold molecular gas that fuels both processes. Studies such as those of Alonso-Herrero et al. [2006] demonstrate that mid-infrared emission provides a robust tracer of star formation in dusty environments, highlighting how complementary wavelengths are required to disentangle gas inflow, star formation, and AGN activity in barred galaxies.

At earlier cosmic times, the role of bars may be fundamentally different. HST-based studies show that the fraction of barred disc galaxies decreases significantly with redshift, particularly for massive systems, indicating that strong bars become common only after galaxies dynamically settle [Melvin et al., 2014]. At the same time, morphological studies of AGN host galaxies at $z \sim 2$ reveal that most moderate-luminosity AGN reside in relatively undisturbed disc galaxies rather than ongoing major mergers, pointing to secular processes as a dominant fuelling mechanism even at high redshift [Kocevski et al., 2012]. These results raise the question of when bars begin to influence AGN activity and whether the bar–AGN connection evolves as discs grow more stable over cosmic time.

The James Webb Space Telescope (JWST) offers a unique opportunity to address this question. JWST's near- and mid-infrared imaging and spectroscopy allow rest-frame optical diagnostics of galaxies at high redshift to be studied with unprecedented sensitivity and spatial resolution [Hickox and Alexander, 2018]. This makes it possible to identify bars in distant galaxies, characterise their host discs, and trace obscured star formation and AGN activity simultaneously. By extending bar–AGN studies into the JWST era, future work can test whether the relationships observed locally persist at earlier epochs, or whether bars only become relevant for AGN fuelling once galaxies reach a later, more dynamically settled stage [Pontoppidan et al., 2022].

Spatially resolved spectroscopy is also essential for studying the internal gas dynamics of barred galaxies. Integral Field Unit (IFU) spectroscopy allows astronomers to obtain a full spectrum at every position across a galaxy, rather than a single spectrum from its centre. As shown by the CALIFA (Calar Alto Legacy Integral Field Area) survey Sánchez et al. [2012], IFU data make it possible to compare central SDSS-like spectra with spectra that represent the entire galaxy, revealing that galaxy classifications and physical properties can depend strongly on aperture size. By providing two-dimensional maps of gas, stars, and kinematics, IFU observations are essential for linking large-scale structures such as bars to the physical processes that govern gas transport and nuclear activity, and for testing whether bars truly drive inflows capable of feeding AGN [Sánchez et al., 2012].

Bibliography

E. L. Alexander. *Magnetic Fields Around Radio Galaxies*. Phd thesis, The University of Manchester, 2022.

Almudena Alonso-Herrero, George H. Rieke, Marcia J. Rieke, Luis Colina, Pablo G. Pérez-González, and Stuart D. Ryder. Near-infrared and star-forming properties of local luminous infrared galaxies. *The Astrophysical Journal*, 650 (2):835, oct 2006. doi: 10.1086/506958. URL `https://doi.org/10.1086/506958`.

Robert Antonucci. Unified models for active galactic nuclei and quasars. *ARA&A*, 31:473–521, January 1993. doi: 10.1146/annurev.aa.31.090193.002353.

AstroWiki. Anatomy of a galaxy. `https://publish.obsidian.md/astrowiki/G.+Galaxies/Anatomy+of+a+Galaxy`. Accessed: 2025-01-29.

E. Athanassoula. The existence and shapes of dust lanes in galactic bars. *MRNAS*, 259:345–364, November 1992. doi: 10.1093/mnras/259.2.345.

E. Athanassoula. What determines the strength and the slowdown rate of bars? *Monthly Notices of the Royal Astronomical Society*, 341(4):1179–1198, June 2003. ISSN 1365-2966. doi: 10.1046/j.1365-8711.2003.06473.x. URL `http://dx.doi.org/10.1046/j.1365-8711.2003.06473.x`.

Joshua Barnes, Lars Hernquist, and Francois Schweizer. Colliding galaxies. *Scientific American*, 265:40–47, August 1991. doi: 10.1038/scientificamerican0891-40.

James Binney and Michael Merrifield. *Galactic Astronomy*, volume 62. Princeton University Press, 1998. ISBN 9780691025650. URL `http://www.jstor.org/stable/j.ctv1nxcw51`.

R. D. Blandford and C. F. McKee. Reverberation mapping of the emission line regions of Seyfert galaxies and quasars. *ApJ*, 255:419–439, April 1982. doi: 10.1086/159843.

R. Buta. The Structure and Dynamics of Ringed Galaxies. IV. Surface Photometry and Kinematics of the Ringed Barred Spiral NGC 6300. *ApJS*, 64:383, June 1987. doi: 10.1086/191199.

C. Marcella Carollo. The Centers of Early- to Intermediate-Type Spiral Galaxies: A Structural Analysis. *ApJ*, 523(2):566–574, October 1999. doi: 10.1086/307753.

Bradley W. Carroll and Dale A. Ostlie. *An introduction to modern astrophysics, Second Edition*. 2017.

J. Chaves-Montero, S. Bonoli, B. Trakhtenbrot, A. Fernández-Centeno, C. Queiroz, L. A. Díaz-García, R. M. González Delgado, A. Hernán-Caballero, C. Hernández-Monteagudo, C. Lópen-Sanjuan, R. Overzier, D. Sobral, L. R. Abramo, J. Alcaniz, N. Benitez, S. Carneiro, A. J. Cenarro, D. Cristóbal-Hornillos, R. A. Dupke, A. Ederoclite, A. Marín-Franch, C. Mendes de Oliveira, M. Moles, L. Sodré, K. Taylor, J. Varela, H. Vázquez Ramió, and T. Civera. Black hole virial masses from single-epoch photometry: The minijpas test case. *A&A*, 660:A95, April 2022. ISSN 1432-0746. doi: 10.1051/0004-6361/202142567. URL `http://dx.doi.org/10.1051/0004-6361/202142567`.

Edmond Cheung, E. Athanassoula, Karen L. Masters, Robert C. Nichol, A. Bosma, Eric F. Bell, S. M. Faber, David C. Koo, Chris Lintott, Thomas Melvin, Kevin Schawinski, Ramin A. Skibba, and Kyle W. Willett. Galaxy zoo: Observing secular evolution through bars*. *The Astrophysical Journal*, 779(2):162, dec 2013. doi: 10.1088/0004-637X/779/2/162. URL `https://doi.org/10.1088/0004-637X/779/2/162`.

SDSS Collaboration, Gautham Adamane Pallathadka, Mojgan Aghakhanloo, James Aird, Andrés Almeida, Singh Amrita, Friedrich Anders, Scott F. Anderson, Stefan Arseneau, Consuelo González Avila, Shir Aviram, Catarina Aydar, Carles Badenes, Jorge K. Barrera-Ballesteros, Franz E. Bauer, Aida Behmard, Michelle Berg, F. Besser, Christian Moni Bidin, Dmitry Bizyaev, Guillermo Blanc, Michael R. Blanton, Jo Bovy, William Nielsen Brandt, Joel R. Brownstein, Johannes Buchner, Esra Bulbul, Joseph N. Burchett,

Leticia Carigi, Joleen K. Carlberg, Andrew R. Casey, Priyanka Chakraborty, Julio Chanamé, Vedant Chandra, Cristina Chiappini, Igor Chilingarian, Johan Comparat, Kevin Covey, Nicole Crumpler, Katia Cunha, Elena D'Onghia, Xinyu Dai, Jeremy Darling, Megan Davis, Nathan De Lee, Niall Deacon, José Eduardo Méndez Delgado, Sebastian Demasi, Mariia Demianenko, Delvin Demke, John Donor, Niv Drory, Monica Alejandra Villa Durango, Tom Dwelly, Oleg Egorov, Evgeniya Egorova, Kareem El-Badry, Mike Eracleous, Xiaohui Fan, Emily Farr, Douglas P. Finkbeiner, Logan Fries, Peter Frinchaboy, Nicola Pietro Gentile Fusillo, Luis Daniel Serrano Félix, Boris Gaensicke, Emma Galligan, Pablo García, Joseph Gelfand, Katie Grabowski, Eva Grebel, Paul J Green, Hannah Greve, Catherine Grier, Emily Griffith, Paloma Guetzoyan, Pramod Gupta, Zoe Hackshaw, Patrick B. Hall, Keith Hawkins, Viola Hegedűs, Saskia Hekker, T. M. Herbst, J. J. Hermes, Lorena Hernández-García, Pranavi Hiremath, David W Hogg, Jon Holtzman, Keith Horne, Danny Horta, Yang Huang, Brian Hutchinson, Maximilian Häberle, Hector Javier Ibarra-Medel, Alexander P. Ji, Paula Jofre, James W. Johnson, Jennifer Johnson, Evelyn J. Johnston, Mary Kaldor, Ivan Katkov, Arman Khalatyan, Sergey Khoperskov, Ralf Klessen, Matthias Kluge, Anton M. Koekemoer, Juna A. Kollmeier, Marina Kounkel, Kathryn Kreckel, Dhanesh Krishnarao, Mirko Krumpe, Ivan Lacerna, Chervin Laporte, Sebastien Lepine, Jing Li, Fu-Heng Liang, Guilherme Limberg, Xin Liu, Sarah Loebman, Knox Long, Yuxi Lu, Madeline Lucey, Alejandra Z. Lugo-Aranda, Mary Loli Martínez Martinez-Aldama, Kevin McKinnon, Ilija Medan, Andrea Merloni, Sean Morrison, Natalie Myers, Szabolcs Mészáros, Johanna Müller-Horn, Samir Nepal, Melissa Ness, David Nidever, Christian Nitschelm, Audrey Oravetz, Jonah Otto, Kaike Pan, Facundo Pérez Paolino, Castalia Alenka Negrete Peñaloza, Marc Pinsonneault, Manuchehr Taghizadeh Popp, Adrian Price-Whelan, Nadiia Pulatova, Anna Barbara Queiroz, Jordan Raddick, Amy Rankine, Hans-Walter Rix, Carlos Román-Zúñiga, Daniela Fernández Rosso, Jessie Runnoe, Serat Mahmud Saad, Mara Salvato, Sebastian F. Sanchez, Natascha Sattler, Andrew Saydjari, Conor Sayres, Kevin Schlaufman, Donald P. Schneider, Axel Schwope, Lucas M. Seaton, Rhys Seeburger, Javier Serna, Sanjib Sharma, Yue Shen, Amaya Sinha, Brian Sizemore, Marzena Sniegowska, Yingyi Song, Diogo Souto, Keivan Stassun, Matthias Steinmetz, Zachary Stone, Alexander Stone-Martinez, Guy S. Stringfellow, Aurora Mata Sánchez, José Sánchez-Gallego, Jonathan Tan, Jamie Tayar, Riley Thai, Ani Thakar, Pierre Thibodeaux, Yuan-Sen Ting, Andrew Tkachenko, Benny Trakhtenbrot, Jose G. Fernandez Trincado, Nicholas Troup, Jonathan R. Trump, Natalie Ulloa, Roeland

P. Van der Marel, Pablo Vera, Sandro Villanova, Jaime Villaseñor, Ji Wang, Zachary Way, Anne-Marie Weijmans, Adam Wheeler, John C. Wilson, Aida Wofford, Tony Wong, Qiaoya Wu, Dominika Wylezalek, Xiang-Xiang Xue, Renbin Yan, Qian Yang, Nadia Zakamska, Eleonora Zari, Gail Zasowski, Grisha Zeltyn, Zheng Zheng, Catherine Zucker, and Rodolfo de J. Zermeño. The nineteenth data release of the sloan digital sky survey, 2025. URL `https://arxiv.org/abs/2507.07093`.

G. Contopoulos and T. Papayannopoulos. Orbits in weak and strong bars. *A&A*, 92(1-2):33–46, December 1980.

Stephane Courteau. Deep r-Band Photometry for Northern Spiral Galaxies. *ApJS*, 103:363, April 1996. doi: 10.1086/192281.

G. de Vaucouleurs. Revised Classification of 1500 Bright Galaxies. *ApJS*, 8:31, April 1963. doi: 10.1086/190084.

Gerard de Vaucouleurs. Classification and Morphology of External Galaxies. *Handbuch der Physik*, 53:275, January 1959. doi: 10.1007/978-3-642-45932-0_7.

O. J. Eggen, D. Lynden-Bell, and A. R. Sandage. Evidence from the motions of old stars that the Galaxy collapsed. *ApJ*, 136:748, November 1962. doi: 10.1086/147433.

B. G. Elmegreen and D. M. Elmegreen. Properties of barred spiral galaxies. *ApJ*, 288:438–455, January 1985. doi: 10.1086/162810.

Peter Erwin and Linda S. Sparke. Double bars, inner disks, and nuclear rings in early-type disk galaxies. *The Astronomical Journal*, 124(1):65, jul 2002. doi: 10.1086/340803. URL `https://doi.org/10.1086/340803`.

Paul B. Eskridge, Jay A. Frogel, Richard W. Pogge, Alice C. Quillen, Roger L. Davies, D. L. DePoy, Mark L. Houdashelt, Leslie E. Kuchinski, Solange V. Ramírez, K. Sellgren, Donald M. Terndrup, and Glenn P. Tiede. The Frequency of Barred Spiral Galaxies in the Near-Infrared. *AJ*, 119(2):536–544, February 2000. doi: 10.1086/301203.

ESO. Artist's impression of the milky way galaxy seen edge-on. `https://www.eso.org/public/images/eso1339a/`, 2013. ESO/NASA/JPL-Caltech; image by M. Kornmesser, R. Hurt.

Matthew J Fahey, Izzy L Garland, Brooke D Simmons, William C Keel, Jesse Shanahan, Alison Coil, Eilat Glikman, Chris J Lintott, Karen L Masters, Ed Moran, Rebecca J Smethurst, Tobias Géron, and Matthew R Thorne. Structural decomposition of merger-free galaxies hosting luminous agns. *Monthly Notices of the Royal Astronomical Society*, 537(4):3511–3524, 02 2025. ISSN 0035-8711. doi: 10.1093/mnras/staf239. URL `https://doi.org/10.1093/mnras/staf239`.

B. L. Fanaroff and J. M. Riley. The morphology of extragalactic radio sources of high and low luminosity. *MRNAS*, 167:31P–36P, May 1974. doi: 10.1093/mnras/167.1.31P.

J.D. Fix. *Astronomy: Journey to the Cosmic Frontier*. McGraw-Hill Higher Education, 2007. ISBN 9780073347219. URL `https://books.google.hn/books?id=Vxi2jgEACAAJ`.

Amelia Fraser-McKelvie, Alfonso Aragón-Salamanca, Michael Merrifield, Karen Masters, Preethi Nair, Eric Emsellem, Katarina Kraljic, Dhanesh Krishnarao, Brett H. Andrews, Niv Drory, and Justus Neumann. SDSS-IV MaNGA: spatially resolved star formation in barred galaxies. *MRNAS*, 495(4):4158–4169, July 2020. doi: 10.1093/mnras/staa1416.

Melanie A. Galloway, Kyle W. Willett, Lucy F. Fortson, Carolin N. Cardamone, Kevin Schawinski, Edmond Cheung, Chris J. Lintott, Karen L. Masters, Thomas Melvin, and Brooke D. Simmons. Galaxy Zoo: the effect of bar-driven fuelling on the presence of an active galactic nucleus in disc galaxies. *MRNAS*, 448(4):3442–3454, April 2015. doi: 10.1093/mnras/stv235.

Izzy Garland. Large-scale bars as a mechanism for triggering AGN. In *Galaxies at Crossroads: Outflows and IMF in the VLT/ELT/ALMA/JWST Era*, page 19, September 2024. doi: 10.5281/zenodo.14901974.

Izzy L. Garland, Matthew J. Fahey, Brooke D. Simmons, Rebecca J. Smethurst, Chris J. Lintott, Jesse Shanahan, Maddie S. Silcock, Joshua Smith, William C. Keel, Alison Coil, Tobias Géron, Sandor Kruk, Karen L. Masters, David O'Ryan, Matthew R. Thorne, and Klaas Wiersema. The most luminous, merger-free AGNs show only marginal correlation with bar presence. *MRNAS*, 522(1):211–225, June 2023. doi: 10.1093/mnras/stad966.

C. Martin Gaskell. What broad emission lines tell us about how active galactic nuclei work. *New Astronomy Reviews*, 53(7–10):140–148, July 2009. ISSN

1387-6473. doi: 10.1016/j.newar.2009.09.006. URL http://dx.doi.org/10.1016/j.newar.2009.09.006.

Jenny E. Greene and Luis C. Ho. Estimating Black Hole Masses in Active Galaxies Using the Hα Emission Line. *ApJ*, 630(1):122–129, September 2005. doi: 10.1086/431897.

Tobias Géron, R J Smethurst, Chris Lintott, Sandor Kruk, Karen L Masters, Brooke Simmons, and David V Stark. Galaxy zoo: stronger bars facilitate quenching in star-forming galaxies. *Monthly Notices of the Royal Astronomical Society*, 507(3):4389–4408, 07 2021. ISSN 0035-8711. doi: 10.1093/mnras/stab2064. URL https://doi.org/10.1093/mnras/stab2064.

Timothy M. Heckman and Philip N. Best. The coevolution of galaxies and supermassive black holes: Insights from surveys of the contemporary universe. *Annual Review of Astronomy and Astrophysics*, 52(1):589–660, August 2014. ISSN 1545-4282. doi: 10.1146/annurev-astro-081913-035722. URL http://dx.doi.org/10.1146/annurev-astro-081913-035722.

Ryan C. Hickox and David M. Alexander. Obscured active galactic nuclei. *Annual Review of Astronomy and Astrophysics*, 56(1):625–671, September 2018. ISSN 1545-4282. doi: 10.1146/annurev-astro-081817-051803. URL http://dx.doi.org/10.1146/annurev-astro-081817-051803.

Luis Ho. Supermassive Black Holes in Galactic Nuclei: Observational Evidence and Astrophysical Consequences. In Sandip K. Chakrabarti, editor, *Observational Evidence for the Black Holes in the Universe*, volume 234 of *Astrophysics and Space Science Library*, page 157, January 1999. doi: 10.1007/978-94-011-4750-7_11.

Luis C. Ho, Alexei V. Filippenko, and Wallace L. W. Sargent. A Search for "Dwarf" Seyfert Nuclei. III. Spectroscopic Parameters and Properties of the Host Galaxies. *ApJS*, 112(2):315–390, October 1997. doi: 10.1086/313041.

Jorge Ernesto Horvath. *High-Energy Astrophysics. A Primer*. Undergraduate Lecture Notes in Physics. Springer, 2022. ISBN 978-3-030-92158-3, 978-3-030-92161-3, 978-3-030-92159-0. doi: 10.1007/978-3-030-92159-0.

E. P. Hubble. *Realm of the Nebulae*. 1936.

Shai Kaspi, Paul S. Smith, Hagai Netzer, Dan Maoz, Buell T. Jannuzi, and Uriel Giveon. Reverberation Measurements for 17 Quasars and the Size-Mass-Luminosity Relations in Active Galactic Nuclei. *ApJ*, 533(2):631–649, April 2000. doi: 10.1086/308704.

Dale D. Kocevski, S. M. Faber, Mark Mozena, Anton M. Koekemoer, Kirpal Nandra, Cyprian Rangel, Elise S. Laird, Marcella Brusa, Stijn Wuyts, Jonathan R. Trump, David C. Koo, Rachel S. Somerville, Eric F. Bell, Jennifer M. Lotz, David M. Alexander, Frederic Bournaud, Christopher J. Conselice, Tomas Dahlen, Avishai Dekel, Jennifer L. Donley, James S. Dunlop, Alexis Finoguenov, Antonis Georgakakis, Mauro Giavalisco, Yicheng Guo, Norman A. Grogin, Nimish P. Hathi, Stéphanie Juneau, Jeyhan S. Kartaltepe, Ray A. Lucas, Elizabeth J. McGrath, Daniel H. McIntosh, Bahram Mobasher, Aday R. Robaina, David Rosario, Amber N. Straughn, Arjen van der Wel, and Carolin Villforth. CANDELS: Constraining the AGN-Merger Connection with Host Morphologies at z ~2. *ApJ*, 744(2):148, January 2012. doi: 10.1088/0004-637X/744/2/148.

J. Kormendy. A morphological survey of bar, lens, and ring components in galaxies: secular evolution in galaxy structure. *ApJ*, 227:714–728, February 1979. doi: 10.1086/156782.

John Kormendy and Ralf Bender. A proposed revision of the hubble sequence for elliptical galaxies. *The Astrophysical Journal*, 464(2):L119, jun 1996. doi: 10.1086/310095. URL `https://doi.org/10.1086/310095`.

John Kormendy and Karl Gebhardt. Supermassive black holes in galactic nuclei. In J. Craig Wheeler and Hugo Martel, editors, *20th Texas Symposium on relativistic astrophysics*, volume 586 of *American Institute of Physics Conference Series*, pages 363–381. AIP, October 2001. doi: 10.1063/1.1419581.

John Kormendy and Luis C. Ho. Coevolution (Or Not) of Supermassive Black Holes and Host Galaxies. *ARA&A*, 51(1):511–653, August 2013. doi: 10.1146/annurev-astro-082708-101811.

John Kormendy and Robert C. Kennicutt, Jr. Secular Evolution and the Formation of Pseudobulges in Disk Galaxies. *ARA&A*, 42(1):603–683, September 2004. doi: 10.1146/annurev.astro.42.053102.134024.

John Kormendy and Douglas Richstone. Inward Bound—The Search For Supermassive Black Holes In Galactic Nuclei. *ARA&A*, 33:581, January 1995. doi: 10.1146/annurev.aa.33.090195.003053.

Gwang-Ho Lee, Jong-Hak Woo, Myung Gyoon Lee, Ho Seong Hwang, Jong Chul Lee, Jubee Sohn, and Jong Hwan Lee. Do Bars Trigger Activity in Galactic Nuclei? *ApJ*, 750(2):141, May 2012. doi: 10.1088/0004-637X/750/2/141.

Lick Observatory. Shane telescope — research telescopes, 2024. URL `https://www.lickobservatory.org/explore/research-telescopes/shane-telescope/`. Accessed: 2025-01-XX.

D. Lynden-Bell and A. J. Kalnajs. On the generating mechanism of spiral structure. *MRNAS*, 157:1, January 1972. doi: 10.1093/mnras/157.1.1.

V. Marels, V. Mesa, M. Jaque Arancibia, S. Alonso, G. Coldwell, G. Damke, and V. Contreras Rojas. The role of bars in triggering active galactic nuclei galaxies, 2025. URL `https://arxiv.org/abs/2505.23958`.

Paul Martini and Richard W. Pogge. [ital]hubble space telescope[/ital][ital]hubble space telescope[/ital] observations of the c[clc]f[/clc]a seyfert 2 galaxies: The fueling of active galactic nuclei. *The Astronomical Journal*, 118(6):2646–2657, December 1999. ISSN 0004-6256. doi: 10.1086/301140. URL `http://dx.doi.org/10.1086/301140`.

Karen L. Masters, Moein Mosleh, A. Kathy Romer, Robert C. Nichol, Steven P. Bamford, Kevin Schawinski, Chris J. Lintott, Dan Andreescu, Heather C. Campbell, Ben Crowcroft, Isabelle Doyle, Edward M. Edmondson, Phil Murray, M. Jordan Raddick, Anže Slosar, Alexander S. Szalay, and Jan Vandenberg. Galaxy Zoo: passive red spirals. *MNRAS*, 405(2):783–799, June 2010. doi: 10.1111/j.1365-2966.2010.16503.x.

Karen L. Masters, Robert C. Nichol, Martha P. Haynes, William C. Keel, Chris Lintott, Brooke Simmons, Ramin Skibba, Steven Bamford, Riccardo Giovanelli, and Kevin Schawinski. Galaxy Zoo and ALFALFA: atomic gas and the regulation of star formation in barred disc galaxies. *MRNAS*, 424(3): 2180–2192, August 2012. doi: 10.1111/j.1365-2966.2012.21377.x.

Thomas Melvin, Karen Masters, Chris Lintott, Robert C. Nichol, Brooke Simmons, Steven P. Bamford, Kevin R. V. Casteels, Edmond Cheung, Edward M. Edmondson, Lucy Fortson, Kevin Schawinski, Ramin A. Skibba,

Arfon M. Smith, and Kyle W. Willett. Galaxy zoo: an independent look at the evolution of the bar fraction over the last eight billion years from hst-cosmos. *Monthly Notices of the Royal Astronomical Society*, 438(4): 2882–2897, 01 2014. ISSN 0035-8711. doi: 10.1093/mnras/stt2397. URL https://doi.org/10.1093/mnras/stt2397.

David Merritt and Laura Ferrarese. The $M_\bullet$-σ Relation for Supermassive Black Holes. *ApJ*, 547(1):140–145, January 2001. doi: 10.1086/318372.

John S. Mulchaey and Michael W. Regan. The fueling of nuclear activity: The bar properties of seyfert and normal galaxies. *The Astrophysical Journal*, 482 (2):L135, jun 1997. doi: 10.1086/310710. URL https://doi.org/10.1086/310710.

Ramesh Narayan. Black holes in astrophysics. *New Journal of Physics*, 7(1): 199, sep 2005. doi: 10.1088/1367-2630/7/1/199. URL https://doi.org/10.1088/1367-2630/7/1/199.

Ramesh Narayan and Insu Yi. Advection-dominated Accretion: A Self-similar Solution. *ApJL*, 428:L13, June 1994. doi: 10.1086/187381.

Ramesh Narayan and Insu Yi. Advection-dominated Accretion: Underfed Black Holes and Neutron Stars. *ApJ*, 452:710, October 1995. doi: 10.1086/176343.

NASA/ESA. Hubble image of the dust disk and central black hole in ngc 4261. https://science.nasa.gov/asset/hubble/dust-disk-fuels-black-hole-in-giant-elliptical-galaxy-ngc-4261/, 1997. Hubble Space Telescope observation.

A. Nemer and J. Goodman. Line Profiles of Forbidden Emission Lines and What They Can Tell Us About Protoplanetary Disk Winds. *ApJ*, 961(1):122, January 2024. doi: 10.3847/1538-4357/ad0a8d.

Hagai Netzer. Revisiting the Unified Model of Active Galactic Nuclei. *ARA&A*, 53:365–408, August 2015. doi: 10.1146/annurev-astro-082214-122302.

S. L. O'Dell. The optical continuum emission of active galactic nuclei. *PASP*, 98:140–147, February 1986. doi: 10.1086/131735.

Sree Oh, Kyuseok Oh, and {Sukyoung K.} Yi. Bar effects on central star formation and active galactic nucleus activity. *Astrophysical Journal, Supplement*

Series, 198(1), January 2012. ISSN 0067-0049. doi: 10.1088/0067-0049/198/1/4.

Daeseong Park, Jong-Hak Woo, Tommaso Treu, Aaron J. Barth, Misty C. Bentz, Vardha N. Bennert, Gabriela Canalizo, Alexei V. Filippenko, Elinor Gates, Jenny E. Greene, Matthew A. Malkan, and Jonelle Walsh. The Lick AGN Monitoring Project: Recalibrating Single-epoch Virial Black Hole Mass Estimates. *ApJ*, 747(1):30, March 2012. doi: 10.1088/0004-637X/747/1/30.

Chien Y. Peng, Luis C. Ho, Chris D. Impey, and Hans-Walter Rix. Detailed Structural Decomposition of Galaxy Images. *AJ*, 124(1):266–293, July 2002. doi: 10.1086/340952.

Ying-jie Peng, Simon J. Lilly, Katarina Kovač, Micol Bolzonella, Lucia Pozzetti, Alvio Renzini, Gianni Zamorani, Olivier Ilbert, Christian Knobel, Angela Iovino, Christian Maier, Olga Cucciati, Lidia Tasca, C. Marcella Carollo, John Silverman, Pawel Kampczyk, Loic de Ravel, David Sanders, Nicholas Scoville, Thierry Contini, Vincenzo Mainieri, Marco Scodeggio, Jean-Paul Kneib, Olivier Le Fèvre, Sandro Bardelli, Angela Bongiorno, Karina Caputi, Graziano Coppa, Sylvain de la Torre, Paolo Franzetti, Bianca Garilli, Fabrice Lamareille, Jean-Francois Le Borgne, Vincent Le Brun, Marco Mignoli, Enrique Perez Montero, Roser Pello, Elena Ricciardelli, Masayuki Tanaka, Laurence Tresse, Daniela Vergani, Niraj Welikala, Elena Zucca, Pascal Oesch, Ummi Abbas, Luke Barnes, Rongmon Bordoloi, Dario Bottini, Alberto Cappi, Paolo Cassata, Andrea Cimatti, Marco Fumana, Gunther Hasinger, Anton Koekemoer, Alexei Leauthaud, Dario Maccagni, Christian Marinoni, Henry McCracken, Pierdomenico Memeo, Baptiste Meneux, Preethi Nair, Cristiano Porciani, Valentina Presotto, and Roberto Scaramella. Mass and Environment as Drivers of Galaxy Evolution in SDSS and zCOSMOS and the Origin of the Schechter Function. *ApJ*, 721(1):193–221, September 2010. doi: 10.1088/0004-637X/721/1/193.

B. M. Peterson, L. Ferrarese, K. M. Gilbert, S. Kaspi, M. A. Malkan, D. Maoz, D. Merritt, H. Netzer, C. A. Onken, R. W. Pogge, M. Vestergaard, and A. Wandel. Central Masses and Broad-Line Region Sizes of Active Galactic Nuclei. II. A Homogeneous Analysis of a Large Reverberation-Mapping Database. *ApJ*, 613(2):682–699, October 2004. doi: 10.1086/423269.

J. E. Peterson and Glen Mackie. A brief history of the astrophysical research consortium and the apache point observatory. *Journal of Astronomical History*

and Heritage, 2006. URL https://api.semanticscholar.org/CorpusID:128954095.

Klaus M. Pontoppidan, Jaclyn Barrientes, Claire Blome, Hannah Braun, Matthew Brown, Margaret Carruthers, Dan Coe, Joseph DePasquale, Néstor Espinoza, Macarena Garcia Marin, Karl D. Gordon, Alaina Henry, Leah Hustak, Andi James, Ann Jenkins, Anton M. Koekemoer, Stephanie LaMassa, David Law, Alexandra Lockwood, Amaya Moro-Martin, Susan E. Mullally, Alyssa Pagan, Dani Player, Charles Proffitt, Christine Pulliam, Leah Ramsay, Swara Ravindranath, Neill Reid, Massimo Robberto, Elena Sabbi, Leonardo Ubeda, Michael Balogh, Kathryn Flanagan, Jonathan Gardner, Hashima Hasan, Bonnie Meinke, and Antonella Nota. The JWST Early Release Observations. *ApJL*, 936(1):L14, September 2022. doi: 10.3847/2041-8213/ac8a4e.

N. Rakić. Kinematics of the H α and H β broad-line region in an SDSS sample of type-1 AGNs. *MRNAS*, 516(2):1624–1634, October 2022. doi: 10.1093/mnras/stac2259.

K. Sakamoto, S. K. Okumura, S. Ishizuki, and N. Z. Scoville. Bar-driven Transport of Molecular Gas to Galactic Centers and Its Consequences. *ApJ*, 525 (2):691–701, November 1999. doi: 10.1086/307910.

S. F. Sánchez, R. C. Kennicutt, A. Gil de Paz, G. van de Ven, J. M. Vílchez, L. Wisotzki, C. J. Walcher, D. Mast, J. A. L. Aguerri, S. Albiol-Pérez, A. Alonso-Herrero, J. Alves, J. Bakos, T. Bartáková, J. Bland-Hawthorn, A. Boselli, D. J. Bomans, A. Castillo-Morales, C. Cortijo-Ferrero, A. de Lorenzo-Cáceres, A. Del Olmo, R.-J. Dettmar, A. Díaz, S. Ellis, J. Falcón-Barroso, H. Flores, A. Gallazzi, B. García-Lorenzo, R. González Delgado, N. Gruel, T. Haines, C. Hao, B. Husemann, J. Iglésias-Páramo, K. Jahnke, B. Johnson, B. Jungwiert, V. Kalinova, C. Kehrig, D. Kupko, Á. R. López-Sánchez, M. Lyubenova, R. A. Marino, E. Mármol-Queraltó, I. Márquez, J. Masegosa, S. Meidt, J. Mendez-Abreu, A. Monreal-Ibero, C. Montijo, A. M. Mourão, G. Palacios-Navarro, P. Papaderos, A. Pasquali, R. Peletier, E. Pérez, I. Pérez, A. Quirrenbach, M. Relaño, F. F. Rosales-Ortega, M. M. Roth, T. Ruiz-Lara, P. Sánchez-Blázquez, C. Sengupta, R. Singh, V. Stanishev, S. C. Trager, A. Vazdekis, K. Viironen, V. Wild, S. Zibetti, and B. Ziegler. CALIFA, the Calar Alto Legacy Integral Field Area survey. I. Survey presentation. *A&A*, 538:A8, February 2012. doi: 10.1051/0004-6361/201117353.

Allan Sandage. On the formation and age of the galaxy. *J. R. Astron. Soc. Can.*, 84:70, April 1990.

J. A. Sellwood and A. Wilkinson. Dynamics of barred galaxies. *Reports on Progress in Physics*, 56(2):173–256, February 1993. doi: 10.1088/0034-4885/56/2/001.

N. I. Shakura and R. A. Sunyaev. Black holes in binary systems. Observational appearance. *A&A*, 24:337–355, January 1973.

Francesco Shankar, David H. Weinberg, Christopher Marsden, Philip J. Grylls, Mariangela Bernardi, Guang Yang, Benjamin Moster, Hao Fu, Rosamaria Carraro, David M. Alexander, Viola Allevato, Tonima T. Ananna, Angela Bongiorno, Giorgio Calderone, Francesca Civano, Emanuele Daddi, Ivan Delvecchio, Federica Duras, Fabio La Franca, Andrea Lapi, Youjun Lu, Nicola Menci, Mar Mezcua, Federica Ricci, Giulia Rodighiero, Ravi K. Sheth, Hyewon Suh, Carolin Villforth, and Lorenzo Zanisi. Probing black hole accretion tracks, scaling relations, and radiative efficiencies from stacked X-ray active galactic nuclei. *MRNAS*, 493(1):1500–1511, March 2020. doi: 10.1093/mnras/stz3522.

Kartik Sheth, Stuart N. Vogel, Michael W. Regan, Michele D. Thornley, and Peter J. Teuben. Secular Evolution via Bar-driven Gas Inflow: Results from BIMA SONG. *ApJ*, 632(1):217–226, October 2005. doi: 10.1086/432409.

Luiz A. Silva-Lima, Lucimara P. Martins, Paula R. T. Coelho, and Dimitri A. Gadotti. Revisiting the role of bars in agn fuelling with propensity score sample matching. *A&A*, 661:A105, May 2022. ISSN 1432-0746. doi: 10.1051/0004-6361/202142432. URL `http://dx.doi.org/10.1051/0004-6361/202142432`.

B. D. Simmons, R. J. Smethurst, and C. Lintott. Supermassive black holes in disc-dominated galaxies outgrow their bulges and co-evolve with their host galaxies. *MRNAS*, 470(2):1559–1569, September 2017. doi: 10.1093/mnras/stx1340.

Alar Toomre. Mergers and Some Consequences. In Beatrice M. Tinsley and Richard B. Gehret Larson, D. Campbell, editors, *Evolution of Galaxies and Stellar Populations*, page 401, January 1977.

C. Megan Urry and Paolo Padovani. Unified Schemes for Radio-Loud Active Galactic Nuclei. *PASP*, 107:803, September 1995. doi: 10.1086/133630.

Marianne Vestergaard and Bradley M. Peterson. Determining Central Black Hole Masses in Distant Active Galaxies and Quasars. II. Improved Optical and UV Scaling Relationships. *ApJ*, 641(2):689–709, April 2006. doi: 10.1086/500572.

A. Wandel, B. M. Peterson, and M. A. Malkan. Central Masses and Broad-Line Region Sizes of Active Galactic Nuclei. I. Comparing the Photoionization and Reverberation Techniques. *ApJ*, 526(2):579–591, December 1999. doi: 10.1086/308017.

Tim Weinzirl, Shardha Jogee, Sadegh Khochfar, Andreas Burkert, and John Kormendy. Bulge n and B/T in High-Mass Galaxies: Constraints on the Origin of Bulges in Hierarchical Models. *ApJ*, 696(1):411–447, May 2009. doi: 10.1088/0004-637X/696/1/411.

B. Willman and J. Strader. "galaxy," defined. *The Astronomical Journal*, 144(3): 76, August 2012. ISSN 1538-3881. doi: 10.1088/0004-6256/144/3/76. URL `http://dx.doi.org/10.1088/0004-6256/144/3/76`.

Donald G. York, J. Adelman, John E. Anderson, Jr., Scott F. Anderson, James Annis, Neta A. Bahcall, J. A. Bakken, Robert Barkhouser, Steven Bastian, Eileen Berman, William N. Boroski, Steve Bracker, Charlie Briegel, John W. Briggs, J. Brinkmann, Robert Brunner, Scott Burles, Larry Carey, Michael A. Carr, Francisco J. Castander, Bing Chen, Patrick L. Colestock, A. J. Connolly, J. H. Crocker, István Csabai, Paul C. Czarapata, John Eric Davis, Mamoru Doi, Tom Dombeck, Daniel Eisenstein, Nancy Ellman, Brian R. Elms, Michael L. Evans, Xiaohui Fan, Glenn R. Federwitz, Larry Fiscelli, Scott Friedman, Joshua A. Frieman, Masataka Fukugita, Bruce Gillespie, James E. Gunn, Vijay K. Gurbani, Ernst de Haas, Merle Haldeman, Frederick H. Harris, J. Hayes, Timothy M. Heckman, G. S. Hennessy, Robert B. Hindsley, Scott Holm, Donald J. Holmgren, Chi-hao Huang, Charles Hull, Don Husby, Shin-Ichi Ichikawa, Takashi Ichikawa, Željko Ivezić, Stephen Kent, Rita S. J. Kim, E. Kinney, Mark Klaene, A. N. Kleinman, S. Kleinman, G. R. Knapp, John Korienek, Richard G. Kron, Peter Z. Kunszt, D. Q. Lamb, B. Lee, R. French Leger, Siriluk Limmongkol, Carl Lindenmeyer, Daniel C. Long, Craig Loomis, Jon Loveday, Rich Lucinio, Robert H. Lupton, Bryan MacKinnon, Edward J. Mannery, P. M. Mantsch, Bruce Margon, Peregrine McGehee, Timothy A. McKay, Avery Meiksin, Aronne Merelli, David G. Monet, Jeffrey A. Munn, Vijay K. Narayanan, Thomas Nash, Eric Neilsen, Rich Neswold, Heidi Jo Newberg, R. C. Nichol, Tom Nicinski, Mario Nonino, Norio Okada, Sadanori Okamura, Jeremiah P. Ostriker, Russell Owen, A. George Pauls, John Peoples,

R. L. Peterson, Donald Petravick, Jeffrey R. Pier, Adrian Pope, Ruth Pordes, Angela Prosapio, Ron Rechenmacher, Thomas R. Quinn, Gordon T. Richards, Michael W. Richmond, Claudio H. Rivetta, Constance M. Rockosi, Kurt Ruthmansdorfer, Dale Sandford, David J. Schlegel, Donald P. Schneider, Maki Sekiguchi, Gary Sergey, Kazuhiro Shimasaku, Walter A. Siegmund, Stephen Smee, J. Allyn Smith, S. Snedden, R. Stone, Chris Stoughton, Michael A. Strauss, Christopher Stubbs, Mark SubbaRao, Alexander S. Szalay, Istvan Szapudi, Gyula P. Szokoly, Anirudda R. Thakar, Christy Tremonti, Douglas L. Tucker, Alan Uomoto, Dan Vanden Berk, Michael S. Vogeley, Patrick Waddell, Shu-i. Wang, Masaru Watanabe, David H. Weinberg, Brian Yanny, Naoki Yasuda, and SDSS Collaboration. The Sloan Digital Sky Survey: Technical Summary. *AJ*, 120(3):1579–1587, September 2000. doi: 10.1086/301513.